The Implementation of Framework for Improvement by Vertical Enhancement (FIVE) into Energy Exascale Earth System Model (E3SM)

Hsiang-He Lee[1*], Peter Bogenschutz[1], and Takanobu Yamaguchi[2,3]

[1]Atmospheric, Earth, and Energy Division, Lawrence Livermore National Laboratory, Livermore, CA, U.S.A.
[2]Cooperative Institute for Research in Environmental Sciences, University of Colorado, Boulder, CO, U.S.A.
[3]NOAA Earth System Research Laboratories, Chemical Sciences Laboratory, Boulder, CO, U.S.A.

Submitted to
Journal of Advances in Modeling Earth Systems

July 2020

*Corresponding author address: Dr. Hsiang-He Lee, 7000 East Avenue, Livermore, CA, 94550, U.S.A.

E-mail: lee1061@llnl.gov

Key points:

- A novel computational framework, FIVE, has been implemented into E3SM and allows select physical processes to be computed on a higher vertical resolution grid.
- When the vertical resolution approaches the LES-like in E3SM-FIVE, the low cloud shows a significant increase of more than 30% in the southeastern Pacific Ocean.
- E3SM-FIVE is much less computationally expensive compared to E3SM with the same high vertical resolution.

Abstract

The low cloud bias in global climate models (GCMs) remains an unsolved problem. Coarse vertical resolution in GCMs has been suggested to be a significant cause of low cloud bias because planetary boundary layer parameterizations cannot resolve sharp temperature and moisture gradients often found at the top of subtropical stratocumulus layers. This work aims to lessen the low cloud problem by implementing a new computational method, the Framework for Improvement by Vertical Enhancement (FIVE), into the Energy Exascale Earth System Model (E3SM). Three physics schemes representing microphysics, radiation, and turbulence as well as vertical advection are interfaced to vertically enhanced physics (VEP), which allows for these processes to be computed on a higher vertical resolution grid compared to the rest of the E3SM model. We demonstrate the better representation of subtropical boundary layer clouds with FIVE while limiting additional computational cost from the increased number of levels. When the vertical resolution approaches the LES-like vertical resolution in VEP, the climatological low cloud amount shows a significant increase of more than 30% in the southeastern Pacific Ocean. Besides the improvement of low-level cloud amount, the skill scores of mid- and high-level cloud amounts are not negatively impacted partly because FIVE can avoid negative consequences of running deep convection parameterization at high vertical resolution.

Plain language summary

Most global climate models (GCMs) underestimate low-level clouds. Increasing vertical resolution in GCMs is one method to solve this problem. In this study, we have implemented a new computational method, known as the Framework for Improvement by Vertical Enhancement (FIVE). FIVE can increase the vertical resolution for select aspects of a global climate model, and in this study, we apply FIVE to the Energy Exascale Earth System Model (E3SM). Our results show that when the vertical resolution approaches 5-10 m, the low cloud amount shows a significant increase of more than 30% in the southeastern Pacific Ocean, while the FIVE method also prevents the simulations from being too computationally expensive.

Keywords

E3SM, FIVE, stratocumulus cloud, vertical resolution, low-level cloud, marine boundary layer

1. Introduction

Accurately representing clouds in weather and climate models is essential. Poor representation of clouds reduces our ability to determine the sign and magnitude of the cloud feedback in climate simulations and to predict temperature and precipitation in weather forecast models correctly. The large low cloud bias in global climate models (GCMs) is a common, persistent issue, which is mainly related to the cloud parameterization problem owing to the keen low-level clouds sensitivity in climate models (Bony & Dufresne, 2005; Nam et al., 2012; Sherwood et al., 2014).

The Cloud Layers Unified By-Binormals (CLUBB) is a modern unified parameterization of planetary boundary layer (PBL), shallow convection, and cloud macrophysics that applies a higher-order closure (HOC) model with assumed probability density functions (PDFs) (Golaz et al., 2007; Larson & Golaz, 2005; Larson et al., 2012). CLUBB predicts turbulence statistics, i.e., higher-order moments, of velocity as well as thermodynamic scalars, and closes the system of equations by assuming a double gaussian PDF composed with updraft and downdraft gaussian PDFs. HOC models including CLUBB have been implemented into GCMs (Bogenschutz et al., 2013; Cheng & Xu, 2015; Guo et al., 2014; Guo et al., 2015; Thayer-Calder et al., 2015) and have improved some degree of representation of boundary layer clouds; e.g., a more steady transition from the stratocumulus regime to the trade cumulus regime (Bogenschutz et al., 2013).

CLUBB has been known to perform best at high vertical resolution. Bogenschutz et al. (2012) showed that single column model (SCM) simulations with CLUBB improved the representation of the stratocumulus and transitional regimes, and these improvements were most pronounced when high vertical resolution was used in the lower troposphere. Bogenschutz et al. (Submitted) (companion paper; henceforth B20) show that coarse vertical resolution in the Energy

Exascale Earth System Model (E3SM) is a significant cause of low cloud bias because CLUBB cannot realize the subgrid scale sharp temperature and moisture gradients often found at the top of subtropical stratocumulus layers. B20 demonstrated that increasing vertical resolution, to that approaching vertical resolutions used in large eddy simulation (LES), in E3SM is a key ingredient towards improving the representation of marine stratocumulus, but comes with excessive computational cost. B20 also pointed out that the Zhang-McFarlane (ZM) deep convection scheme (Zhang & McFarlane, 1995) in E3SM is sensitive to higher vertical resolution and/or time step, resulting in degrading the climate simulation in certain regimes and potentially negating the benefits of higher vertical resolution. An intelligent method that uses higher vertical resolution to obtain optimal performance of a PBL scheme, while minimizing degradations due to other parameterizations in GCMs is desired to negate both computational expense and to avoid running parameterizations which are not designed to run at such high vertical resolution.

Yamaguchi et al. (2017) (henceforth Y17) have developed a method, the Framework for Improvement by Vertical Enhancement (FIVE), which focuses on running parameterizations, such as CLUBB, on the higher vertical resolutions. The concept of FIVE is to create a separate computational domain, in which prognostic variables are allocated on a locally high-resolution grid. FIVE predicts prognostic variables by computing selected one-dimensional (1-D) processes on the locally high-resolution grid (e.g., microphysics, radiation, turbulence, and vertical advection) as well as applying interpolated tendencies from the host model for other processes. The host model predicts their prognostic variables by applying averaged tendencies computed on the locally high-resolution grid. One advantage of FIVE is that high resolution information is kept at all times during the simulation. In Y17, the prototype FIVE has demonstrated superior results for SCM and two-dimensional regional model simulations compared to those performed with low vertical resolution in the host regional model. The prototype FIVE produced results comparable to those performed with a high vertical resolution regional model while saving computational cost.

In this study, we demonstrate that high vertical resolution for certain physical processes is a crucial component towards the improved climatological representation of low-level clouds in large scale models such as E3SM. The purpose of this work is to implement FIVE into E3SM, which is also the first time that such a framework has been implemented into a global model. In addition to large-scale vertical advection, three physics schemes are interfaced with FIVE, which allows for these schemes to be computed on a higher vertical resolution grid compared to the rest of the E3SM model. A brief description of FIVE and E3SM, as well as numerical experiments, are given in Section 2. Simulated results are discussed in Section 3. A further discussion, including the importance of large-scale vertical advection in E3SM-FIVE, time step sensitivity, as well as future potential applications of FIVE, is given in Section 4. The summary is provided in Section 5.

2. Model description and numerical experiments

2.1. Framework for Improvement by Vertical Enhancement (FIVE)

FIVE predicts variables by computing selected 1-D processes (e.g., microphysics, radiation, turbulence, and vertical advection) on the locally high-resolution grid as well as applying interpolated tendencies from the host model for other processes. The embedded process calculations and predictions on the local high-resolution grid are called Vertically Enhanced Physics (VEP). The VEP calculations do not interfere with the order of the computation of processes in the host model (Figure 1) so that the calculation processes are not repeated between the host model and VEP. The averaged tendency calculated in VEP is applied to the host model for prediction. The synchronization between the host model and VEP by exchanging tendencies with one another is necessary to prevent any drift in the host model state. Because FIVE can keep any information in both host model and VEP states, they are conveniently used for tendency calculations.

2.2. E3SM and the selected physics schemes for VEP

The Department of Energy (DOE) E3SM coupled model version 1 is recently released to the community, and a detailed description of E3SM is documented in Golaz et al. (2019). E3SM originated from a version of the CESM1 (Hurrell et al., 2013) and the atmosphere component of E3SMv1, E3SM Atmosphere Model (EAM) (Rasch et al., 2019), is a descendant of the Community Atmosphere Model version 5.3 (CAM5.3) (Neale et al., 2010). EAM uses a spectral element (SE) dynamical core at a 110-km resolution on a cubed sphere geometry and a traditional hybridized sigma pressure vertical coordinate. The transition between terrain following and constant pressure coordinate is made at ~200 hPa (~11km).

The vertical resolution in EAM is 72 layers with a top at approximately 60 km in altitude, which is higher than CAM5.3 with 30 vertical layers and a top at approximately 40 km in altitude. Fifteen layers reside between the surface and 850 hPa ($\Delta Z \approx 25$ m at the surface and $\Delta Z \approx 125$ m near 850 hPa) in EAM, with relatively finer vertical layers, compared to CAM5.3, with the goal to better capture thin clouds and sharp gradients at the top of the boundary layer. Between 850 and 500 hPa the vertical grid spacing is gradually increased from 100 to 500 m because strong water vapor gradients are frequently observed to occur at vertical scales of 500 m or less for important cloud features. This vertical resolution is needed for aerosol plume transport as well. Resolution from the free troposphere (above 500 hPa) up to the lower stratosphere (70 hPa) is increased from 600 to 1200 m to allow for adequate representation of upward propagating large-scale tropical waves such as Kelvin and mixed-Rossby gravity.

Compared to CAM5.3, higher vertical resolution in EAM can better capture thin clouds, sharp gradients at the top of the boundary layer, rapid changes in process rates in microphysics and radiation (autoconversion, accretion, evaporation, and radiative heating rates), and cloud properties (drop size and rain rates); however, the underestimated liquid water content in marine stratocumulus still needs further improvement, consistent with other GCMs. Despite the increases in vertical resolution in E3SM compared to CAM, B20 found that the vertical resolution of about 10 m is needed in the lower troposphere to resolve the sharp gradients at stratocumulus top. E3SM falls well below meeting these criteria. However, running at such high vertical resolution for all of E3SM is prohibitively expensive for long climate simulations and can result in degradation of the climate simulation when running schemes not designed for high vertical resolution.

Y17 identified the essential processes for successful stratocumulus simulations, which should be computed with high vertical resolution. In their study, they used a single column model to test microphysics, radiation, turbulence, and vertical advection (i.e., subsidence). Their results show that microphysics needs to be processed in VEP because it includes vertical transport in the form of cloud water sedimentation and rainwater precipitation. They also suggested computing vertical advection in VEP because the bias associated with subsidence (same as sedimentation) produces higher PBL depth, which results in a warmer and dryer PBL by entrainment. Turbulence parameterization in the host model resolution is too weak to mix the variability, so neglecting turbulence parameterization in VEP results in a particularly noisy profile in the host model. Turbulence parameterization in VEP can effectively smooth the variation developed in VEP.

Radiation can be computed outside VEP provided that the interpolated radiative heating rate at the cloud top is accurately captured.

Following Y17, in addition to large-scale vertical advection discussed below, three physics schemes in EAM are selected for VEP to be run at higher vertical resolution to better represent low clouds:

1. Cloud Layers Unified By Binormals (CLUBB) is a third-order turbulence closure parameterization that unifies the treatment of planetary boundary layer turbulence, shallow convection, and cloud macrophysics (Golaz et al., 2002; Larson & Golaz, 2005).
2. Morrison and Gettelman microphysics scheme version 2 (MG2) is a two-moment microphysics scheme to predict the number concentrations and mixing ratios of liquid and ice particles (Gettelman et al., 2015; Morrison & Gettelman, 2008).
3. Rapid Radiative Transfer Model for GCMs (RRTMG) longwave and shortwave radiation schemes use a modified correlated-k method to calculate radiative fluxes and heating rates in the clear sky and for condensed phase species (Iacono et al., 2008; Mlawer et al., 1997).

Before the start of these physics schemes in VEP, the tendency profile from the host model is interpolated to the VEP vertical grid to obtain the synchronized tendency profile between the host model and VEP for computing the process with the local high-resolution profiles (Figure 1). Then, prognostic and diagnostic variables are calculated on the locally high-resolution grid and high-resolution information is kept at all times among the processes (i.e., turbulence, microphysics, and radiation). For example, cloud fraction is diagnosed by the CLUBB parameterization at high vertical resolution, which is saved and then passed to the microphysics and radiation parameterizations, instead of interpolating this variable back from the E3SM vertical grid. Finally, the averaged prognostic tendencies computed at high vertical resolution (as in VEP) from the selected three physics schemes are applied to the host model for prediction.

2.3. Large-scale vertical advection adjustment

Besides the physics schemes, Y17 found it crucial that large-scale vertical advection be computed on the high resolution grid. This is necessary to accurately balance entrainment via the turbulence scheme. Note that unlike the other processes, this calculation occurs in the dynamical core in EAM. EAM uses sigma pressure vertical coordinate and the vertically Lagrangian approach from Lin (2004). At the beginning of each time step, the tracers, as well as temperature and horizontal wind components, are assumed to be given on the sigma coordinate layer mid points. The tracers are advanced in time on a moving vertical coordinate system as a floating point. At the end of the time step, the tracers are remapped back to the sigma coordinate layer mid points using the monotone remap algorithm from Zerroukat et al. (2005). With the existing remapping algorithm in E3SM, all tracers with the high vertical resolution are also remapped back to the FIVE sigma coordinate layer for large-scale vertical advection adjustment at the end of the time step. The importance of large-scale vertical advection in FIVE for E3SM is discussed in Section 4.1.

2.4. Model configuration and numerical experiment design

The purpose of this experiment design is to see whether the representation of marine stratocumulus is improved when the vertical resolution in VEP increases for the selected physical processes (i.e., CLUBB, MG microphysics scheme, and RRTMG radiation scheme) and large-scale vertical advection. Note that all other processes are computed on the standard 72-layer grid. The configuration of the model control run (CNTL) is based on the configuration of E3SMv1, 110-km horizontal resolution (ne30), and 72 vertical layers. Four principal simulations were designed to double (FIVE_DOUB), quadruple (FIVE_QUAD), octuple (FIVE_OCT), and sexdecuple (FIVE_SEXDEC) vertical resolution of VEP between 995 hPa and 700 hPa (Table 1). The vertical grid configurations for VEP are identical to the grid configuration of the E3SM benchmark experiments (DOUB, QUAD, OCT, and SEXDEC) in B20 (companion paper), where vertical resolution was increased in the lower troposphere for the entire model. The comparison of E3SM benchmark experiments and E3SM-FIVE runs is presented in Section 3.3. Similar to B20, none of our FIVE experiments were tuned in anyway.

Although a time step reduction is necessary for a stable benchmark OCT run, FIVE_OCT does not need a time step reduction. To help elucidate any sensitivities arising from time step differences between FIVE simulations and benchmark runs, two additional simulations, FIVE_OCT_t150 and FIVE_OCT_d900, have been performed. We reduced the CLUBB and microphysics time step from 300 s to 150 s for FIVE_OCT_t150 and the dynamics time step from 1800 s to 900 s for FIVE_OCT_d900, which is the same time step set up as the benchmark OCT experiment. Note that the dynamics time step remains unmodified, relative to CNTL, for all simulations besides FIVE_OCT_d900 (Table 2).

Another simulation, FIVE_OCT_noLS, was designed as a sensitivity test for the effects of large-scale vertical advection on the high vertical resolution grid. FIVE_OCT_noLS means no large-scale vertical advection is computed in FIVE (i.e., it is computed on the standard 72 layer grid), but three selected physics schemes remain coupled to FIVE. The duration of all principal simulations are 5 years and the sensitivity runs (FIVE_OCT_t150, FIVE_OCT_d900, and FIVE_OCT_noLS) are integrated for 2 years. Tables 1 and 2 summarize the grid configuration and time step settings for our principle and sensitivity experiments.

3. Results

3.1. E3SM control run

As previously mentioned, E3SM has higher vertical resolution, compared to CAM5.3, with the expectation that it would better represent marine stratocumulus. However, the stratocumulus biases are similar in the two models, so further improvements to the low-level cloud amount and shortwave cloud radiative effect (SWCRE) biases are needed in E3SM. Figure 2a shows the climatologically averaged low-level cloud amount from Cloud-Aerosol Lidar and Infrared Pathfinder Satellite Observation (CALIPSO) lidar data from January 2007 to January 2010. Low stratiform clouds are primarily found over the oceans and those clouds can be classified into three types of stratiform clouds by Klein and Hartmann (1993): stratiform clouds on the east side of the oceanic subtropical highs, stratocumulus clouds form over the warm western boundary currents in winter, and Arctic stratus.

In order to conduct apples-to-apples comparisons, our E3SM simulations use the Cloud Feedback Model Intercomparing Project (CFMIP) Observation Simulator Package (COSP; Bodas-Salcedo et al. (2011)) when evaluating simulated low cloud climatology with observations. Compared to CALIPSO, CNTL captures a general pattern of low-level cloud amount (Figure 2b), and the correlation between CNTL and observation can be as high as 0.87. The underestimated low-level cloud amount in CNTL mainly appears in the tropical and subtropical regions. The biases over eastern oceans, e.g., Eastern Pacific Ocean, Eastern Atlantic Ocean, and Eastern Indian Ocean, can be more than a 30% deficit (Figure 2c). The stratiform clouds over these regions occur in response to trade winds blowing from mid-latitudes toward the intertropical convergence zone (ITCZ). These clouds form over oceans with relatively cool sea surface temperature associated with ocean upwelling circulation and form a strong temperature inversion that caps the boundary layer. As the air in the trade winds approaches the ITCZ and warmer water, the trade inversion generally rises and weakens, and trade wind cumulus convection replaces the stratiform clouds.

Owing to the underestimated low-level cloud amount in CNTL, the SWCRE biases also appear over the corresponding areas of eastern oceans compared to the observation (Figure 3c). The observational data of SWCRE is from the Clouds and the Earth's Radiant Energy System (CERES) Energy Balanced and Filled (EBAF) top-of-atmosphere (TOA) data product averaged from 2000 to 2015 (Figure 3a). It should be noted that the maximum SWCRE biases are ruled by not only low cloud amount but also solar insolation, so that the variation of SWCRE is quite high from season to season.

3.2. E3SM-FIVE results

In this section, we focus on the improvements of low cloud gained with FIVE relative to the control run (CNTL). Figure 4 shows that compared to CNTL, the biases associated with low-level cloud amount are gradually improved with E3SM-FIVE simulations in eastern oceans when we increase the VEP vertical resolution, especially in the eastern Pacific Ocean. It is interesting to note that the improvement of the low-level cloud amount in FIVE_DOUB is negligible, while modest improvements are seen in FIVE_QUAD with increases of the low-level cloud amount around 5-10% in the tropical and subtropical regions. When the vertical resolution approaches LES-like resolutions in the FIVE_OCT and FIVE_SEXDEC experiments, the low-level cloud amount is significantly increased.

It is important to note that the reduction of low cloud amount biases with increasing vertical resolution is consistent with the results of the companion study (Figure 3 in B20), which found that LES-like vertical resolution is necessary to achieve significant improvements in the low cloud climatology. Compared to CNTL, the low-level cloud amounts in FIVE_OCT and

FIVE_SEXDEC are increased by more than 30% in the southeastern Pacific Ocean. The improvement of low cloud biases for offshore stratocumulus (or "core" regions as defined in Klein and Hartmann (1993)) appears to mostly converge with vertical resolution between FIVE_OCT and FIVE_SEXDEC simulations. B20 is not able to address whether their SEXDEC simulation led to better results compared to their OCT simulation because their SEXDEC simulation required extreme time step adjustment, which introduced large sensitivity (discussed in Section 3.3). Since E3SM-FIVE does not need time step reduction, we can conclude that going from LES-like vertical resolutions of FIVE_OCT to FIVE_SEXDEC does not appear to lead to significant improvements for offshore stratocumulus, but appears to lead to some improvements for coastal low-level cloud amount (Figure 4d).

The SWCRE biases are also gradually improved in the corresponding marine stratocumulus areas with increasing resolution of VEP, especially in the southeast Pacific Ocean (Figure 5). Our simulations show that the improvement of low cloud biases first appears in the offshore "core" regions as vertical resolution increases, but not along the coasts. The maximum biases of the low-level cloud in CNTL, however, occur in the coastal area, such as the west coast of North America and South America (Figure 1c). Only in FIVE_SEXDEC is the improvement of low cloud biases along the coasts more visible (Figure 5d). Our result shows that increasing vertical resolution toward LES-like vertical resolutions indeed improves the simulation of stratocumulus along the coastal regions in a global climate model.

Furthermore, FIVE_SEXDEC predicts less low-level cloud amount over the polar regions than CNTL, which has not been seen in the other FIVE simulations. The SWCRE over the polar regions in FIVE_SEXDEC is also simulated higher than that in CNTL (Figure 5d). B20 (companion study) presented a similar feature in the benchmark OCT run and speculated a potential sensitivity of CLUBB, MG2, or their interactions to high vertical resolution in the presence of mixed phase clouds and/or the stable boundary layer (Figures 3 and 6 in B20). In their benchmark simulations, OCT resulted in significant differences in liquid water path (LWP) and ice water path (IWP) in the polar regions compared to other lower vertical resolution benchmark cases. Higher LWP and lower IWP in the Antarctic Circle (~60ºS in latitude), and lower LWP and no change IWP in the north polar regions in OCT (Figure 12 in B20) contribute to a slightly weaker SWCRE in the polar regions, which is closer to the observation. In our simulations, both LWP and IWP in FIVE_SEXDEC are lower than those in other E3SM-FIVE simulations (Figure 6a and 6b), which weakens not only SWCRE but also longwave cloud radiative effect (LWCRE) in FIVE_SEXDEC in the polar regions (Figure 6c and 6d). Among the E3SM-FIVE and E3SM benchmark simulations, FIVE_SEXDEC has SWCRE and LWCRE best comparable to the observation (Table 6). This weaker SWCRE in FIVE_SEXDEC compensates the negative biases in the polar regions of CNTL against the observation (Figure 3c). Figure 7 shows the differences of SWCRE between E3SM-FIVE simulations and observation. Overall, the results in FIVE_SEXDEC show improvement compared to the observations, even in the polar area (Figure 7d). The sensitivity to vertical resolution in the polar regions is interesting but beyond the scope of this work; we leave in depth investigation to future work.

This study focuses on the improvement of low stratiform clouds by increasing vertical resolution in the lower troposphere for select processes. Besides presenting the effects on the global low cloud climatology, we also focus on the five subtropical marine stratus regions for detailed analyses. Based on the definition of stratus regions in Klein and Hartmann (1993), Table 3 shows the selected regions, their locations and the seasons of maximum stratus that we analyze.

Figure 8a and 8b display that the cloud fraction and cloud liquid amount in the Peruvian region increase along with the total number of vertical layers in the E3SM-FIVE simulations, while climatological cloud top height and cloud thickness both increase as well. The maximum cloud fraction in CNTL resides at ~880 hPa, while the peak of the cloud fraction profile in all E3SM-FIVE simulations is about 20 hPa higher (~860 hPa). Compared to observations, all E3SM-FIVE experiments simulate too little cloud fraction and too thin cloud depth; however, they produce a peak cloud liquid water amount that is fairly comparable to observations. Here, the observational data is provided by CALIPSO, CloudSat, and Moderate Resolution Imaging Spectroradiometer (MODIS) in a merged product called C3M (Kato et al., 2010). The minimum peak of the longwave cloud heating rate profile in all E3SM-FIVE simulations is also 20 hPa higher than in CNTL (Figure 8c). Besides that, the discrepancy of each longwave heating profile among E3SM-FIVE simulations is small. It is worthwhile to mention that FIVE_DOUB and FIVE_QUAD have similar results compared to the profiles of benchmark DOUB and QUAD in B20 over the Peruvian region. However, the peak cloud fraction and cloud liquid amount are predicted 30% higher in OCT than FIVE_OCT.

The cloud fraction over the Californian region decreases in FIVE_DOUB and then increases along with the vertical resolution in the E3SM-FIVE simulations, while cloud top height and cloud thickness both increase as well (Figure 8d). The peak of cloud liquid amount in all E3SM-FIVE simulations tends to be 20~30 hPa higher than the peak in observations (Figure 8e). Compared to CNTL, FIVE_SEXDEC is the only simulation showing some improvement in the cloud fraction and cloud liquid amount. We notice that the peak magnitude of cloud fraction in FIVE_SEXDEC is similar to the result in the benchmark OCT as well as the peak magnitude of cloud liquid amount and cloud top height (Figure 9 in B20). The longwave cloud heating rate in

FIVE_SEXDEC also has the highest simulated cooling rates among all E3SM-FIVE simulations (Figure 8f).

The improvements in cloud fraction over the Namibian region (Figure 8g), which is a fairly active and strong stratocumulus regime, are similar to Peruvian (c.f., Figure 8a). The results for Australian and Canarian also show better representation with FIVE compared to CNTL; though perhaps relatively more muted. It may be because these regions typically are not characterized by as strong inversions or high cloud cover, hence subject somewhat less sensitivity to vertical resolution, than the other regions.

3.3. The comparison of E3SM-FIVE and E3SM benchmarks

3.3.1. Computational cost

B20 gradually increased the vertical resolution for the entire E3SM model from 135 m to 15 m at climatologically typical stratocumulus inversion height, same as the experiment designs in this study. In previous LES studies, 5 to 10 m vertical resolution is recommended to resolve the inversion (Bretherton et al., 1999; Stevens et al., 2005). The benchmark simulations in B20 show that the improvement of low cloud biases has become conspicuous only when the vertical resolution approaches the LES resolution. The improvement of low cloud biases in DOUB (70 m vertical resolution) was negligible, while marginal impacts were seen in QUAD (35 m vertical resolution) for low cloud biases, especially in the southeastern Pacific Ocean and the southeastern Atlantic Ocean.

Increasing vertical resolution is a necessary ingredient to improve low cloud amount; however, using LES-like vertical resolution for the entire model is expensive. Table 4 shows the comparison of computational cost between the E3SM benchmarks and E3SM-FIVE simulations. The computational cost of the benchmark runs is exponentially increased with the total number of layers, partially owing to the fact that the OCT and SEXDEC benchmark runs required a reduction of time step.

In comparison, running FIVE_DOUB is slightly slower than running DOUB. The current prototype version of E3SM-FIVE has not yet been optimized. Further optimization tests are needed in the future to reduce the overhead costs of E3SM-FIVE. FIVE_QUAD is run with the same time step settings as QUAD but requests less the computational cost. In FIVE_QUAD, the overhead cost of FIVE is not as large as the expense of running horizontal advection and other high vertical resolution physics schemes, which are not computed in FIVE (e.g., deep convection scheme). Furthermore, a significant performance advantage is found when running at LES-Like vertical resolutions in E3SM-FIVE, which is partially because no time step decrease is required in any E3SM-FIVE simulations (Table 1). FIVE_OCT is about four times faster than OCT, while the savings of FIVE_SEXDEC is more than an order of magnitude than SEXDEC.

These timing numbers represent a significant advantage for E3SM-FIVE runs. For instance, B20 was unable to run their SEXDEC experiment for longer than two years; while we were able to report on a five-year simulation of FIVE-SEXDEC without undue computational burden.

3.3.2. Comparison of climatology

Figure 9 shows the differences of low-level cloud amount between the E3SM benchmarks and the E3SM-FIVE experiments. Compared to the E3SM-FIVE simulations, the increases of low-level cloud amount in the benchmarks are more significant along with the total number of vertical layers. However, benchmarks and E3SM-FIVE simulations, compared to observations, both have shown an improvement of low-level cloud amount. We want to highlight that the benchmark OCT run overestimated the low-level cloud amount in the offshore region of Peruvian by 20-25% (Figure 2 in B20) and it also results in too strong SWCRE over this region.

Table 5 shows the root mean square error (RMSE) and bias of low-level cloud amount for three extended stratocumulus regions defined in Table 3 in each benchmark and E3SM-FIVE run against observations. In terms of RMSE, the three regions generally show increasing skill in the benchmarks for each region as resolution increases, while the OCT simulation performs the best for all regions. For the E3SM-FIVE simulations, besides FIVE_SEXDEC, other simulations follow the trend of increasing skill as resolution increases. For the Peruvian and Namibian regions, the OCT simulation is an outlier in the regards showing a net positive bias, which is not seen in any E3SM-FIVE simulations. Although compared to the benchmarks, the E3SM-FIVE simulations have higher RMSE and bias of low cloud amount in the stratocumulus regions, overall low cloud climatology for these regions is improved with FIVE.

The global RMSE of low-level cloud amount in each benchmark and E3SM-FIVE run against observations is listed in Table 6. When the vertical resolution increases, both benchmarks and E3SM-FIVE have shown a declining trend of RMSE biases of low-level cloud amount. Overall, benchmarks still have a better result in the low-level cloud amount than the E3SM-FIVE runs. While E3SM-FIVE runs overall show similar behavior in the representation of low cloud climatology compared to benchmark runs (i.e., generally as vertical resolution increases, low cloud amount increases), it is worthwhile to discuss potential reasons why there are some differences in the magnitude between these runs. Potential reasons could be i) differences in the simulated Hadley circulation due to feedbacks from not running the ZM deep convection scheme at high vertical resolution in E3SM-FIVE, and ii) errors associated with the tendency interpolation for synchronization between E3SM and VEP (i.e., losing accuracy versus in a free running simulation).

Compared to the observation, the RMSE of SWCRE in benchmarks also show a downward trend when the vertical resolution increases (Table 6). However, when the vertical resolution approaches 15 m in OCT, the errors of SWCRE increase again. The rebound trend of RMSE of SWCRE does not appear in E3SM-FIVE. Although the RMSE of SWCRE in the E3SM-FIVE runs are higher than that in the benchmarks, the declining trend is more consistent along with the increase of vertical resolution. Figure 10 shows the differences of SWCRE between the E3SM benchmarks and the E3SM-FIVE experiments. In general, FIVE_OCT has stronger SWCRE compared to OCT (higher negative value in Figure 10c). As mentioned previously, the overestimated low-level cloud amount and SWCRE over the offshore region of Peruvian are present in OCT. FIVE_OCT leads better results in this region (Figure 9c and 10c). B20 found that OCT has too weak SWCRE over the tropical regions and also reported that the ZM deep convection scheme is sensitive to the higher vertical resolution and/or time step, which leads to a degradation in the climate simulation over the deep convective tropics. Since E3SM-FIVE does not run the ZM deep convection scheme at high vertical resolution, we avoid the negative consequences of running parameterizations that may not be designed to run at such high vertical resolution; which is another benefit of FIVE (Figure 7).

Compared to observations, the RMSE of precipitation in the E3SM-FIVE runs are not distinguishable from each other and the RMSE in the benchmarks increases along with the vertical resolution, owing to the sensitivity of the deep convection scheme to high vertical resolution (Table 6). We further demonstrate this by examining the degradation of precipitation in the OCT simulation reported by B20. Figure 11 shows that compared to the precipitation biases in FIVE_OCT, the biases of precipitation in OCT are higher in the tropical regions. B20 found that when the vertical resolution increases, the large-scale precipitation rate gradually increases and the convective precipitation rate declines (Figure 11 in B20). With their analysis, it was not clear if this shift in partitioning and degradation of precipitation skill scores as vertical resolution increases represents a sensitivity coming from the ZM deep convection scheme itself or due to a sensitivity arising from the CLUBB and/or microphysical parameterization. In the E3SM-FIVE simulations, large-scale precipitation rate slightly increases when the vertical resolution increases, but no obvious sensitivity is found in convective precipitation rate (Figure 12). This suggests that the strong sensitivity and poor skill scores demonstrated by the OCT simulation in B20 stems from a sensitivity of the ZM deep convection scheme to vertical resolution and/or time step rather than a sensitivity arising in the CLUBB turbulence scheme and/or the MG2 microphysics scheme.

The RMSE of mid-level cloud amount, high-level cloud amount, and LWCRE, for each experiment in E3SM benchmarks and E3SM-FIVE against the observations are also presented in Table 6. Although the benchmark runs improve low-level cloud amount compared to CNTL, the RMSE of mid- and high-level cloud amount get worse with higher vertical resolution. On the other hand, while E3SM-FIVE improves low-level cloud amount compared to CNTL and in a similar manner compared to benchmarks, the skill scores of mid- and high-level cloud amount are not negatively impacted. Similar to the RMSE of SWCRE, the RMSE of LWCRE in benchmarks shows a downward trend when the vertical resolution increases, but the biases of LWCRE increase again in OCT. The rebound trend of RMSE of LWCRE, again, does not appear in E3SM-FIVE. Our results show global skill of both LWCRE and SWCRE do not exhibit degradation with respect to vertical resolution in E3SM-FIVE because these simulations are not subjected to sensitivities of the ZM scheme at high vertical resolution.

4. Discussion

4.1. The importance of large-scale vertical advection in FIVE

As mentioned in Section 2.3, the large-scale vertical advection computed in FIVE is necessary to balance entrainment via turbulence scheme. Figure 13 shows the comparison of FIVE_OCT and FIVE_OCT_noLS to quantify the impact of the large-scale vertical advection in FIVE. Figure 13a shows without the adjustment of vertical advection in FIVE, the low-level cloud amount is reduced as much as 10%, especially in the marine stratocumulus regions. These differences also are found in the SWCRE (Figure 13b). Consistent with Y17, this test indeed shows that all four processes (i.e., microphysics, radiation, turbulence, and large-scale vertical advection) need to be applied on the VEP grid for a reasonable match with the benchmark simulations and observations.

4.2. CFL condition in E3SM-FIVE

As previously mentioned, a big performance advantage found in E3SM-FIVE is that when running at LES-like vertical resolutions, no time step reduction is required. This is counter to B20, in which their high vertical resolution benchmark simulations were subject to time stepping constraints. This brings into question the Courant-Friedrichs-Lewy (CFL) condition for stable numerical integration of partial differential equations. Normally, the CFL condition should be considered for explicit time integration schemes to set an appropriate time step size. E3SM-FIVE is not constrained by the CFL condition because most of the physics schemes selected for VEP are implicit.

The CLUBB turbulence scheme and the MG2 microphysics scheme use an implicit scheme and time-split sedimentation, respectively. The vertical advection uses a semi-Lagrangian scheme, so it is not subject to time step limitation either. Generally, the implicit scheme uses the entire domain to calculate each time step, and implicit calculations at each time step are computational expensive. It is worthwhile to mention that the time step constraint in the benchmarks is associated with the ZM deep convection scheme, which has been tested in a sensitivity simulation in B20. They found that their OCT simulation ran stably with ZM shut off, with CLUBB acting as a deep convection parameterization, with default model time steps.

4.3. Time step sensitivity test

Previous studies demonstrated that climate variables in GCMs are sensitive to model time step, especially those associated with deep and shallow convective parameterization (Williamson, 2013; Yu & Pritchard, 2015). Williamson (2013) suggested that many of these sensitivities maybe due to convective parameterization schemes failing to effectively adjust moist instability by vertical redistribution and associated condensation when the adjustment timescales assumed in convective parameterizations are longer than a GCM time step. B20 also demonstrated that their high resolution benchmark simulations were sensitive to time step settings and they concluded that these sensitivities may arise from the ZM deep convection scheme.

An additional test is performed to see if CLUBB and MG2 have a time step sensitivity at high vertical resolution. Figure 14a and 14b show that the differences of low-level cloud amount between FIVE_OCT_t150 (in which CLUBB and microphysics time steps were reduced from 300 s to 150 s) and FIVE_OCT are negligible, while there are some minor differences of SWCRE between FIVE_OCT_t150 and FIVE_OCT in Southeast Asia, which does not show a significant sensitivity in the low-cloud regions we are focused on. Overall, reducing time step in CLUBB and microphysics schemes does not substantially affect the long-term climate trend nor the climatological stratocumulus results.

The results for FIVE_OCT_d900 (the experiment where E3SM time step was reduced from 1800 s to 900 s) also provide a similar conclusion. Figure 14c shows the differences of low-level cloud amount between FIVE_OCT_d900 and FIVE_OCT. We reduced the time step of E3SM dynamics and physics by half, but the low-level cloud amount has no significant changes compared to FIVE_OCT, only small increases in the intertropical convergence zone. Minor differences of SWCRE between FIVE_OCT_d900 and FIVE_OCT also show a scattering distribution pattern, but weaker SWCRE in FIVE_OCT_d900 is over Australia (Figure 14d). The RMSE scores of precipitation for FIVE_OCT_t150 and FIVE_OCT_d900 are 1.21 and 1.23 mm day^{-1}, respectively, computed relative to the observations. Compared to the RMSE in FIVE_OCT (1.14 mm day^{-1}), the results in FIVE_OCT_t150 and FIVE_OCT_d900 are slightly higher but not as high as the RMSE in OCT (1.66 mm day^{-1}; Table 6). Overall, our results show that E3SM-FIVE is not sensitive to time step.

These results also suggest that the large sensitivities seen in the tropics for the OCT simulation in B20 are related to sensitivities in the vertical resolution rather than the model time step, arising from the ZM deep convection scheme.

4.4. Future applications of FIVE

Significant computational savings is one of the main benefits for using E3SM-FIVE. The total cost is less than the benchmark runs, especially at LES-like high vertical resolutions where we see substantial improvements in the simulation of marine stratocumulus. However, costs quickly mount when the number of VEP levels increases; even if no time step decrease is required (Table 4). The current version of E3SM-FIVE uses a common fixed VEP grid for all columns. Since the cost associated with FIVE is tightly related to the number of VEP levels, we expect that the VEP cost burden can be reduced by applying a variant of the Adaptive Vertical Grid (AVG) method (Marchand & Ackerman, 2011) to the VEP grid. The AVG scheme in E3SM-FIVE is an on-going project, which aims to allow the vertical extent of the high resolution region and the number of vertical levels of the high resolution region of the VEP grid in each column to dynamically adapt as the solution evolves.

Our current highest vertical resolution results still show less stratocumulus in the coastal regions of California and Peru, compared to observations, and we hypothesize that these deficiencies probably require concurrent increases in horizontal and vertical resolution. One potential application of FIVE is to use regional refinement in the horizontal over stratocumulus regions (Tang et al., 2019). By this method we would have concurrent horizontal and vertical resolution increases, but only in the regions where they are desired to reduce the computational cost.

On the other hand, FIVE could also be applied to super-parameterized (SP) GCMs (Grabowski, 2001; M. Khairoutdinov et al., 2005; M. F. Khairoutdinov & Randall, 2001; Randall et al., 2003) so that the embedded cloud resolving model runs at higher vertical resolution while keep the host GCM runs at the standard vertical resolution. SP tries to address shortcomings of conventional GCMs by embedding small cloud-resolving models in each global model grid column. Marchand and Ackerman (2010) investigated the cloud cover in a 1 km horizontal grid resolution of an embedded cloud system resolving model used in SP GCMs and the results show higher horizontal resolution decreased low cloud cover. However, increasing vertical resolution with higher horizontal resolution helped to restore low-cloud cover and modestly improved cloud-top height.

Typical SP implementations have used cloud-resolving models with 1-4 km horizontal resolution and a coarse vertical resolution encompassing 30-50 vertical layers, which have not been able to resolve the turbulent eddies that form low cloud due to grid resolution limitations. While this has produced promising effects for deep convection, it is known that accurate representation of cloud-top-entrainment plays a crucial role in the realistic simulation of low clouds. This requires extremely fine vertical grid spacing (5-25 m) and horizontal drip spacing (5-100 m)(Grabowski, 2016). Thus, applying FIVE in SP can serve the purpose of finer vertical resolution in the CRM to accurately simulate turbulence and entrainment processes near sharp temperature inversions, but retaining the relatively coarse vertical resolution for the host model to reduce computational cost.

5. Summary

The aim of this work is to implement a new computational method, the Framework for Improvement by Vertical Enhancement (FIVE), into the Energy Exascale Earth System Model (E3SM). Three physics schemes, the CLUBB turbulence scheme, the MG2 microphysics scheme, and the RRTMG radiation schemes as well as vertical advection, are interfaced to vertically enhanced physics (VEP), which allows for these schemes to be computed on a higher vertical resolution grid compared to the rest of the E3SM model. This is the first time, to our knowledge, that such a framework has been applied to a GCM. For our proof of concept implementation, we focus on the climatological effects of the marine stratocumulus regime, since this is a regime that is known to be sensitive to vertical resolution.

Three physics schemes are essential in E3SM-FIVE for high vertical resolution in successful stratocumulus simulations owing to the tight interaction between turbulence, microphysics, and radiation. Besides the physics schemes, using FIVE in the large-scale vertical advection in the dynamic core is necessary to balance entrainment via the turbulence scheme, and in our sensitivity study, it can increase the low cloud amount by ~10% in the marine stratocumulus regions, as well as ameliorating radiational biases.

In this paper, we used VEP for turbulence, microphysics, radiation parameterizations, and vertical advection, and demonstrated the better representation of subtropical boundary layer clouds. The configuration of the control run (CNTL) is based on the configuration of E3SMv1 (72 vertical layers). Four principal simulations were designed to double (FIVE_DOUB; 92 vertical layers), quadruple (FIVE_QUAD; 132 vertical layers), octuple (FIVE_OCT; 212 vertical layers) and sexdecuple (FIVE_SEXDEC; 372 vertical layers) the vertical resolution between 995 hPa and 700 hPa. The purpose of the experimental design is to see how the representation of marine stratocumulus is improved when the high vertical resolution is applied to select physical processes.

Our results show when the vertical resolution approaches LES-like resolutions in FIVE_OCT and FIVE_SEXDEC, the low cloud amount shows a significant increase of more than 30% in the southeastern Pacific Ocean and the improvement seems to converge at these scales. The shortwave cloud radiative effect has also been improved as well in the corresponding area, mostly in the southeast Pacific Ocean. Our simulations show that the improvement of low-level cloud bias focuses on the offshore "core" regions but not along the coasts. The improvement of the low-level cloud bias along the coasts becomes visible only in FIVE_SEXDEC. It is unclear if further vertical refinement would lead to further decreases in biases in these regions, but we speculate that concurrent increases in horizontal and vertical resolution are needed to significantly ameliorate coastal stratocumulus biases.

Compared to the E3SM benchmarks, E3SM-FIVE limits additional computational cost from the increased number of levels, especially when running at LES-like vertical resolutions. No reduction of E3SM time step is required with any of the E3SM-FIVE configurations, compared to the E3SM benchmark runs, which is partially why E3SM-FIVE greatly reduces computational cost compared with high vertical simulations without FIVE. The time step constraint in the benchmark simulations is concluded to be associated with the Zhang-McFarlance (ZM) deep convection scheme, which has been tested in a benchmark sensitivity simulation (see Bogenschutz et al. (Submitted)). The ZM deep convection scheme is sensitive to higher vertical resolution, and it results in a degrading climate simulation in the deep convective tropics. In sensitivity tests, our prototype E3SM-FIVE is not sensitive to time step and free from the CFL condition. In other words, in E3SM-FIVE, we can avoid negative consequences of running parameterizations which may be negatively impacted by higher vertical resolution.

Regarding future applications of FIVE, we discussed an ongoing project for adaptive vertical grid for the VEP grid, for cost mitigation, which allows the vertical extent of the high-resolution region and the number of vertical levels of the high-resolution region of the VEP grid in each column to dynamically adapt as the solution evolves. FIVE and horizontal mesh refinement is one potential application of FIVE to concurrently increase in horizontal and vertical resolution over stratocumulus regions. Another application of FIVE is in regard to the embedded cloud resolving models (CRMs) in super-parameterization, where the idea is to increase the vertical resolution of the embedded CRM, but not of the host model.

Finally, although this paper focuses on the marine stratocumulus regime for our proof of concept implementation, the application of FIVE in E3SM is not limited to the lower troposphere. For example, one could increase the vertical resolution in VEP to the upper troposphere to examine the effects of vertical resolution on cirrus clouds.

Code and data availability:

The model code used in this study is located at https://doi.org/10.5281/zenodo.3893210. The output from the E3SM-FIVE simulations can be found at https://doi.org/10.5281/zenodo.3887276.

Acknowledgements:

This work was funded by Scientific Discovery through Advanced Computing (SciDAC; Award number: DE-SC0018650) by the U.S. Department of Energy office of Biological and Environment Research. Work at LLNL was performed under the auspices of the U.S. DOE by Lawrence Livermore National Laboratory under contract DE-AC52-07NA27344. LLNL IM: LLNL-JRNL-810691-DRAFT.

References:

Bodas-Salcedo, A., Webb, M. J., Bony, S., Chepfer, H., Dufresne, J.-L., Klein, S. A., . . . John, V. O. (2011). COSP: Satellite simulation software for model assessment. *Bulletin of the American Meteorological Society, 92*(8), 1023-1043. doi:10.1175/2011bams2856.1

Bogenschutz, P. A., Gettelman, A., Morrison, H., Larson, V. E., Craig, C., & Schanen, D. P. (2013). Higher-Order Turbulence Closure and Its Impact on Climate Simulations in the Community Atmosphere Model. *Journal of Climate, 26*(23), 9655-9676. doi:10.1175/JCLI-D-13-00075.1

Bogenschutz, P. A., Gettelman, A., Morrison, H., Larson, V. E., Schanen, D. P., Meyer, N. R., & Craig, C. (2012). Unified parameterization of the planetary boundary layer and shallow convection with a higher-order turbulence closure in the Community Atmosphere Model: single-column experiments. *Geosci. Model Dev., 5*(6), 1407-1423. doi:10.5194/gmd-5-1407-2012

Bogenschutz, P. A., Yamaguchi, T., & Lee, H. H. (Submitted). E3SM Simulations with High Vertical Resolution in the Lower Troposphere. *Journal of Advances in Modeling Earth Systems*.

Bony, S., & Dufresne, J.-L. (2005). Marine boundary layer clouds at the heart of tropical cloud feedback uncertainties in climate models. *Geophysical Research Letters, 32*(20). doi:10.1029/2005gl023851

Bretherton, C. S., Macvean, M. K., Bechtold, P., Chlond, A., Cotton, W. R., Cuxart, J., . . . Wyant, M. C. (1999). An intercomparison of radiatively driven entrainment and turbulence in a smoke cloud, as simulated by different numerical models. *Quarterly Journal of the Royal Meteorological Society, 125*(554), 391-423. doi:10.1002/qj.49712555402

Cheng, A., & Xu, K.-M. (2015). Improved Low-Cloud Simulation from the Community Atmosphere Model with an Advanced Third-Order Turbulence Closure. *Journal of Climate, 28*(14), 5737-5762. doi:10.1175/jcli-d-14-00776.1

Gettelman, A., Morrison, H., Santos, S., Bogenschutz, P., & Caldwell, P. M. (2015). Advanced Two-Moment Bulk Microphysics for Global Models. Part II: Global Model Solutions and

Aerosol–Cloud Interactions. *Journal of Climate, 28*(3), 1288-1307. doi:10.1175/jcli-d-14-00103.1

Golaz, J.-C., Caldwell, P. M., Van Roekel, L. P., Petersen, M. R., Tang, Q., Wolfe, J. D., . . . Zhu, Q. (2019). The DOE E3SM Coupled Model Version 1: Overview and Evaluation at Standard Resolution. *Journal of Advances in Modeling Earth Systems, 11*(7), 2089-2129. doi:10.1029/2018ms001603

Golaz, J.-C., Larson, V. E., & Cotton, W. R. (2002). A PDF-Based Model for Boundary Layer Clouds. Part I: Method and Model Description. *Journal of the Atmospheric Sciences, 59*(24), 3540-3551. doi:10.1175/1520-0469(2002)059<3540:APBMFB>2.0.CO;2

Golaz, J.-C., Larson, V. E., Hansen, J. A., Schanen, D. P., & Griffin, B. M. (2007). Elucidating Model Inadequacies in a Cloud Parameterization by Use of an Ensemble-Based Calibration Framework. *Monthly Weather Review, 135*(12), 4077-4096. doi:10.1175/2007mwr2008.1

Grabowski, W. W. (2001). Coupling Cloud Processes with the Large-Scale Dynamics Using the Cloud-Resolving Convection Parameterization (CRCP). *Journal of the Atmospheric Sciences, 58*(9), 978-997. doi:10.1175/1520-0469(2001)058<0978:Ccpwtl>2.0.Co;2

Grabowski, W. W. (2016). Towards Global Large Eddy Simulation: Super-Parameterization Revisited. *Journal of the Meteorological Society of Japan. Ser. II, 94*(4), 327-344. doi:10.2151/jmsj.2016-017

Guo, H., Golaz, J.-C., Donner, L. J., Ginoux, P., & Hemler, R. S. (2014). Multivariate Probability Density Functions with Dynamics in the GFDL Atmospheric General Circulation Model: Global Tests. *Journal of Climate, 27*(5), 2087-2108. doi:10.1175/JCLI-D-13-00347.1

Guo, H., Golaz, J.-C., Donner, L. J., Wyman, B., Zhao, M., & Ginoux, P. (2015). CLUBB as a unified cloud parameterization: Opportunities and challenges. *Geophysical Research Letters, 42*(11), 4540-4547. doi:10.1002/2015gl063672

Hurrell, J. W., Holland, M. M., Gent, P. R., Ghan, S., Kay, J. E., Kushner, P. J., . . . Marshall, S. (2013). The Community Earth System Model: A Framework for Collaborative Research. *Bulletin of the American Meteorological Society, 94*(9), 1339-1360. doi:10.1175/bams-d-12-00121.1

Iacono, M. J., Delamere, J. S., Mlawer, E. J., Shephard, M. W., Clough, S. A., & Collins, W. D. (2008). Radiative forcing by long-lived greenhouse gases: Calculations with the AER radiative transfer models. *Journal of Geophysical Research: Atmospheres, 113*(D13). doi:10.1029/2008jd009944

Kato, S., Sun-Mack, S., Miller, W. F., Rose, F. G., Chen, Y., Minnis, P., & Wielicki, B. A. (2010). Relationships among cloud occurrence frequency, overlap, and effective thickness derived from CALIPSO and CloudSat merged cloud vertical profiles. *Journal of Geophysical Research: Atmospheres, 115*(D4). doi:10.1029/2009jd012277

Khairoutdinov, M., Randall, D., & DeMott, C. (2005). Simulations of the Atmospheric General Circulation Using a Cloud-Resolving Model as a Superparameterization of Physical Processes. *Journal of the Atmospheric Sciences, 62*(7), 2136-2154. doi:10.1175/jas3453.1

Khairoutdinov, M. F., & Randall, D. A. (2001). A cloud resolving model as a cloud parameterization in the NCAR Community Climate System Model: Preliminary results. *Geophysical Research Letters, 28*(18), 3617-3620. doi:10.1029/2001gl013552

Klein, S. A., & Hartmann, D. L. (1993). The Seasonal Cycle of Low Stratiform Clouds. *Journal of Climate, 6*(8), 1587-1606. doi:10.1175/1520-0442(1993)006<1587:Tscols>2.0.Co;2

Larson, V. E., & Golaz, J.-C. (2005). Using Probability Density Functions to Derive Consistent Closure Relationships among Higher-Order Moments. *Monthly Weather Review, 133*(4), 1023-1042. doi:10.1175/mwr2902.1

Larson, V. E., Schanen, D. P., Wang, M., Ovchinnikov, M., & Ghan, S. (2012). PDF Parameterization of Boundary Layer Clouds in Models with Horizontal Grid Spacings from 2 to 16 km. *Monthly Weather Review, 140*(1), 285-306. doi:10.1175/mwr-d-10-05059.1

Lin, S.-J. (2004). A “Vertically Lagrangian” Finite-Volume Dynamical Core for Global Models. *Monthly Weather Review, 132*(10), 2293-2307. doi:10.1175/1520-0493(2004)132<2293:Avlfdc>2.0.Co;2

Marchand, R., & Ackerman, T. (2010). An analysis of cloud cover in multiscale modeling framework global climate model simulations using 4 and 1 km horizontal grids. *Journal of Geophysical Research: Atmospheres, 115*(D16). doi:10.1029/2009jd013423

Marchand, R., & Ackerman, T. (2011). A Cloud-Resolving Model with an Adaptive Vertical Grid for Boundary Layer Clouds. *Journal of the Atmospheric Sciences, 68*(5), 1058-1074. doi:10.1175/2010jas3638.1

Mlawer, E. J., Taubman, S. J., Brown, P. D., Iacono, M. J., & Clough, S. A. (1997). Radiative transfer for inhomogeneous atmospheres: RRTM, a validated correlated-k model for the longwave. *Journal of Geophysical Research: Atmospheres, 102*(D14), 16663-16682. doi:10.1029/97jd00237

Morrison, H., & Gettelman, A. (2008). A New Two-Moment Bulk Stratiform Cloud Microphysics Scheme in the Community Atmosphere Model, Version 3 (CAM3). Part I: Description and Numerical Tests. *Journal of Climate, 21*(15), 3642-3659. doi:10.1175/2008jcli2105.1

Nam, C., Bony, S., Dufresne, J.-L., & Chepfer, H. (2012). The ‘too few, too bright’ tropical low-cloud problem in CMIP5 models. *Geophysical Research Letters, 39*(21). doi:10.1029/2012gl053421

Neale, R., Gettelman, A., Park, S., Chen, C., Lauritzen, P., Williamson, D., . . . Smith, A. (2010). Description of the NCAR Community Atmosphere Model (CAM 5.0), NCAR Tech. Note TN-486. *Boulder, CO: National Center for Atmospheric Research*.

Randall, D., Khairoutdinov, M., Arakawa, A., & Grabowski, W. (2003). Breaking the Cloud Parameterization Deadlock. *Bulletin of the American Meteorological Society, 84*(11), 1547-1564. doi:10.1175/bams-84-11-1547

Rasch, P. J., Xie, S., Ma, P.-L., Lin, W., Wang, H., Tang, Q., . . . Yang, Y. (2019). An Overview of the Atmospheric Component of the Energy Exascale Earth System Model. *Journal of Advances in Modeling Earth Systems, 11*(8), 2377-2411. doi:10.1029/2019ms001629

Sherwood, S. C., Bony, S., & Dufresne, J.-L. (2014). Spread in model climate sensitivity traced to atmospheric convective mixing. *Nature, 505*(7481), 37-42. doi:10.1038/nature12829

Stevens, B., Moeng, C.-H., Ackerman, A. S., Bretherton, C. S., Chlond, A., Roode, S. d., . . . Zhu, P. (2005). Evaluation of Large-Eddy Simulations via Observations of Nocturnal Marine Stratocumulus. *Monthly Weather Review, 133*(6), 1443-1462. doi:10.1175/mwr2930.1

Tang, Q., Klein, S. A., Xie, S., Lin, W., Golaz, J. C., Roesler, E. L., . . . Zheng, X. (2019). Regionally refined test bed in E3SM atmosphere model version 1 (EAMv1) and applications for high-resolution modeling. *Geosci. Model Dev., 12*(7), 2679-2706. doi:10.5194/gmd-12-2679-2019

Thayer-Calder, K., Gettelman, A., Craig, C., Goldhaber, S., Bogenschutz, P. A., Chen, C. C., . . . Ghan, S. J. (2015). A unified parameterization of clouds and turbulence using CLUBB and subcolumns in the Community Atmosphere Model. *Geosci. Model Dev., 8*(12), 3801-3821. doi:10.5194/gmd-8-3801-2015

Williamson, D. L. (2013). The effect of time steps and time-scales on parametrization suites. *Quarterly Journal of the Royal Meteorological Society, 139*(671), 548-560. doi:10.1002/qj.1992

Yamaguchi, T., Feingold, G., & Larson, V. E. (2017). Framework for improvement by vertical enhancement: A simple approach to improve representation of low and high-level clouds in large-scale models. *Journal of Advances in Modeling Earth Systems, 9*(1), 627-646. doi:10.1002/2016MS000815

Yu, S., & Pritchard, M. S. (2015). The effect of large-scale model time step and multiscale coupling frequency on cloud climatology, vertical structure, and rainfall extremes in a superparameterized GCM. *Journal of Advances in Modeling Earth Systems, 7*(4), 1977-1996. doi:10.1002/2015ms000493

Zerroukat, M., Wood, N., & Staniforth, A. (2005). A monotonic and positive–definite filter for a Semi-Lagrangian Inherently Conserving and Efficient (SLICE) scheme. *Quarterly Journal of the Royal Meteorological Society, 131*(611), 2923-2936. doi:10.1256/qj.04.97

Zhang, G. J., & McFarlane, N. A. (1995). Sensitivity of climate simulations to the parameterization of cumulus convection in the Canadian climate centre general circulation model. *Atmosphere-Ocean, 33*(3), 407-446. doi:10.1080/07055900.1995.9649539

Table 1. Principle experiment designs for this study. The second column is the total vertical layers. The third and fourth column are the time step set up for E3SM dynamic and the time step for CLUBB and microphysics in each simulation run, respectively. All principle experiments are performed 5 years in length.

FIVE runs	Layers	E3SM time step (seconds)	CLUBB and microphysics time step (seconds)
CNTL	72	1800	300
FIVE_DOUB	92	1800	300
FIVE_QUAD	132	1800	300
FIVE_OCT	212	1800	300
FIVE_SEXDEC	372	1800	300

Table 2. Sensitivity experiment designs for this study. The second column is the total vertical layers. The third and fourth column are the time step set up for E3SM dynamic and the time step for CLUBB and microphysics in each simulation run, respectively. All sensitivity experiments are performed 2 years in length.

FIVE runs	Layers	E3SM time step (seconds)	CLUBB and microphysics time step (seconds)
FIVE_OCT_t150	212	1800	150
FIVE_OCT_d900	212	900	150
FIVE_OCT_noLS	212	1800	300

Table 3. The five status regions, the season of maximum stratiform clouds, and their geographical location (core area) referred to the definition in Klein and Hartmann (1993). SON indicates September, October, and November, etc. The extended area is defined for the analysis in Table 6.

Region	Season of maximum stratus	Location (core area)	Location (extended area)
Peruvian	SON	10º-20ºS, 90º-100ºW*	5º-35ºS, 80º-110ºW
Californian	JJA	20º-30ºN, 120º-130ºW	10º-40ºN, 116º-145ºW
Namibian	SON	10º-20ºS, 0º-10ºE	5º-35ºS, 15ºW-15ºE
Australian	DJF	25º-35ºS, 95º-105ºE	/
Canarian	JJA	15º-25ºS, 25º-35ºW	/

*Location of Peruvian was defined to 0º-20ºS, 80º-90ºW in Klein and Hartmann (1993).

Table 4. The comparison of computational cost between simulations in E3SM-benchmarks and E3SM-FIVE. SYPD indicates simulated years per day.

Benchmarks	CNTL	DOUB	QUAD	OCT	SEXDEC
E3SM-Benchmarks (SYPD / 1024 cores)	4.3	2.2	1.2	0.23	0.03
E3SM-FIVE (SYPD / 1024 cores)	N/A	1.8	1.6	1.21	0.67

Table 5. Root mean squared errors (RMSE) and bias computed relative to CALIPSO observations for the low cloud amounts for three extended stratocumulus regions (Table 3) for each experiment in E3SM benchmarks and E3SM-FIVE against the observations.

	E3SM-Benchmarks				**E3SM-FIVE**			
RMSE	CNTL	DOUB	QUAD	OCT	DOUB	QUAD	OCT	SEXDEC
Peruvian	23.8	19.2	19.3	10.2	21.0	18.2	14.0	16.9
California	26.2	24.8	19.2	12.3	27.6	22.6	19.6	16.4
Namibia	20.5	18.9	7.5	7.3	20.3	14.0	11.4	12.1
	E3SM-Benchmarks				**E3SM-FIVE**			
Bias	CNTL	DOUB	QUAD	OCT	DOUB	QUAD	OCT	SEXDEC
Peruvian	-19.2	-14.5	-12.2	2.6	-18.7	-13.7	-8.4	-12.4
California	-22.5	-19.8	-14.8	-5.7	-24.8	-19.5	-15.9	-14.0
Namibia	-19.0	-14.9	-2.5	2.7	-18.0	-10.8	-6.5	-8.3

Table 6. Root mean square error (RMSE) biases of low-level cloud amount (%), mid-level cloud amount (%), high-level cloud amount (%), shortwave cloud radiative effect (W/m^2), longwave cloud radiative effect (W/m^2), and precipitation (mm/day) for each experiment in E3SM benchmarks and E3SM-FIVE against the observations.

	E3SM-Benchmarks				**E3SM-FIVE**			
	CNTL	DOUB	QUAD	OCT	DOUB	QUAD	OCT	SEXDEC
Low-level cloud amount (%)	12.75	11.90	11.21	10.18	12.73	11.50	11.36	11.01
Mid-level cloud amount (%)	7.32	7.31	7.52	7.96	7.28	7.26	7.28	7.13
High-level cloud amount (%)	7.87	8.00	7.99	9.00	7.95	7.91	7.84	7.81
Shortwave cloud radiative effect (W/m^2)	9.54	9.50	8.98	9.31	9.72	9.45	9.35	8.63
Longwave cloud radiative effect (W/m^2)	8.43	8.19	8.04	9.00	8.84	8.24	8.05	8.06
Precipitation (mm/day)	1.06	1.14	1.36	1.66	1.12	1.15	1.14	1.15

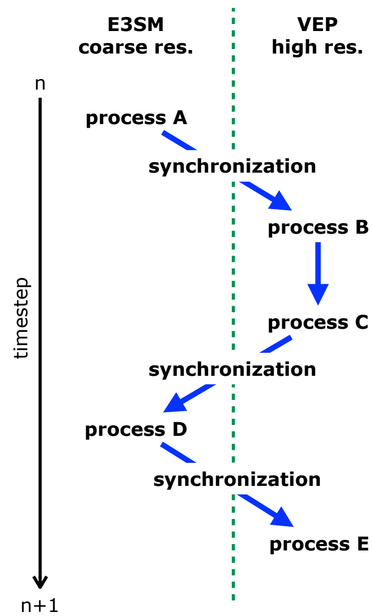

Figure 1. Schematic of the sequence of the processes between the host model (e.g., E3SM) and selected Vertically Enhanced Physics (VEP). For this example, if the sequence of processes in the host model is A, B, C, D, and E, and processes B, C, and E are selected for calculation within VEP, then the order will be: process A (host model) → process B (VEP) → process C (VEP) → process D (host model) → process E (VEP).

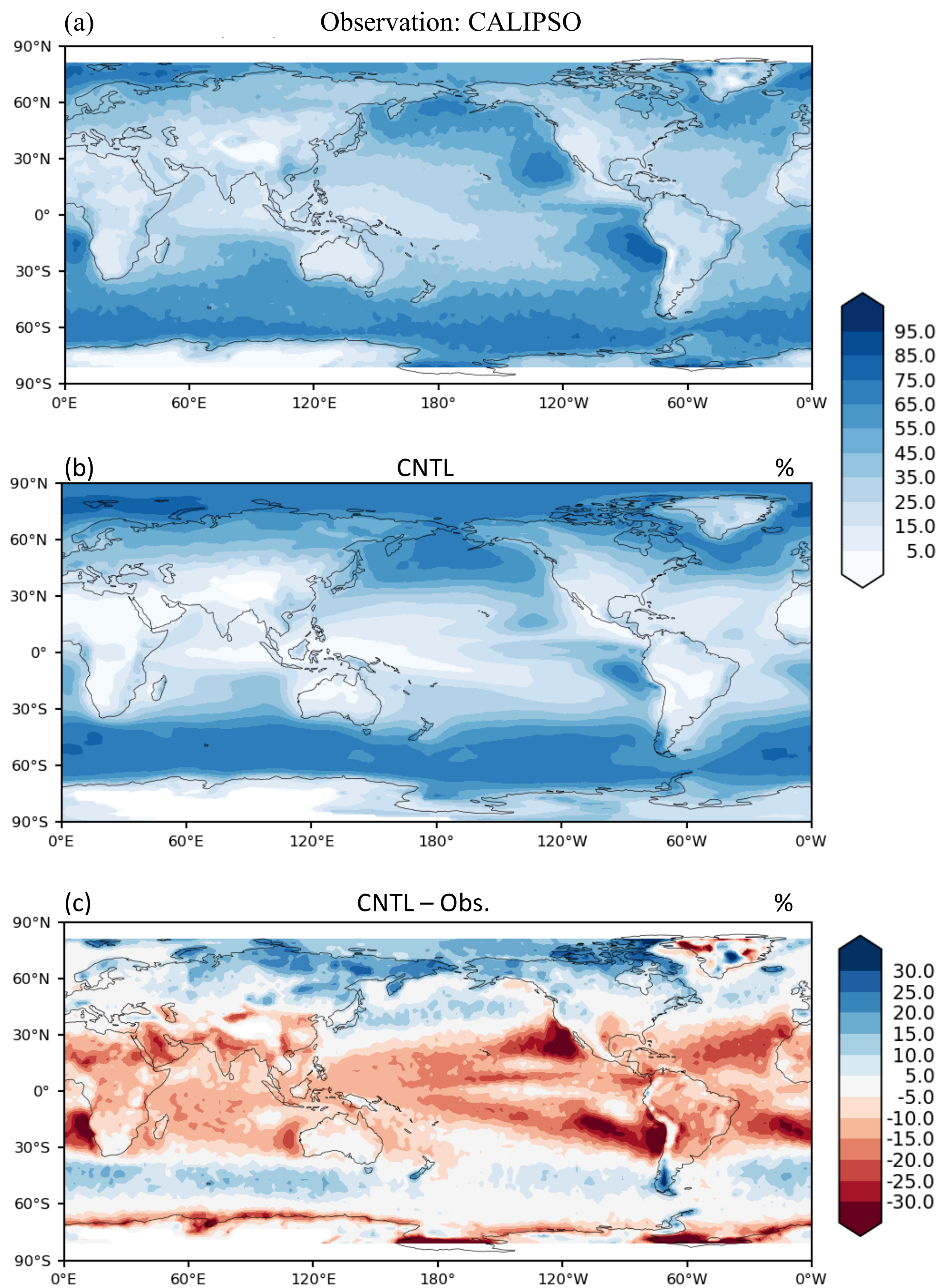

Figure 2. (a) Low level cloud amount from Cloud-Aerosol Lidar and Infrared Pathfinder Satellite Observation (CALIPSO) lidar data from January 2007 to January 2010. (b) Averaged low cloud amount in the control run (CNTL). (c) The differences of low level cloud amountbetween CNTL and observation.

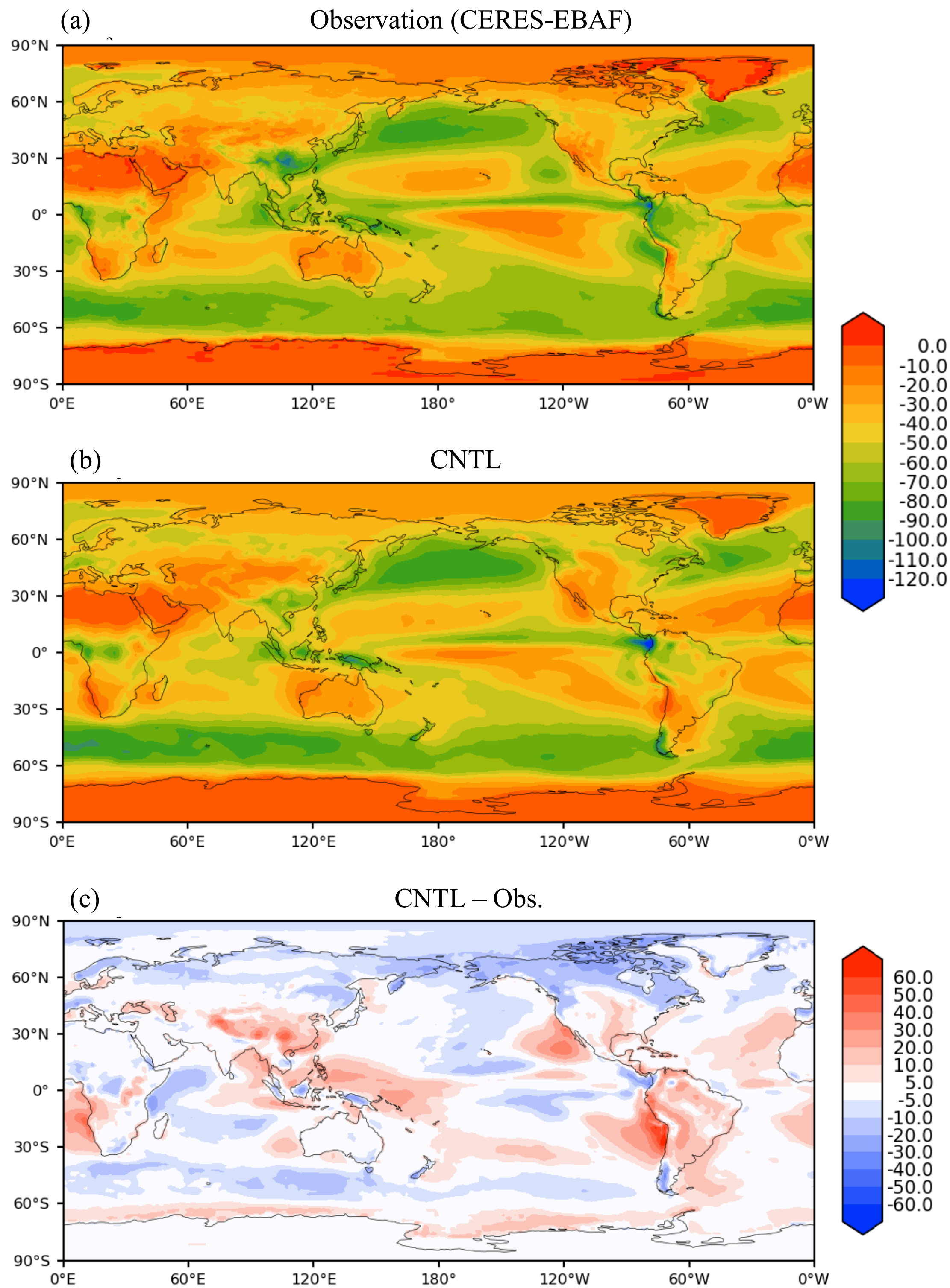

Figure 3. (a) Shortwave cloud radiative effect from the Clouds and the Earth's Radiant Energy System (CERES) Energy Balanced and Filled (EBAF) top-of-atmosphere (TOA) data product averaged from 2000 to 2015. (b) Averaged shortwave cloud radiative effect in the control run (CNTL). (c) The differences of shortwave cloud radiative effect between CNTL and observation.

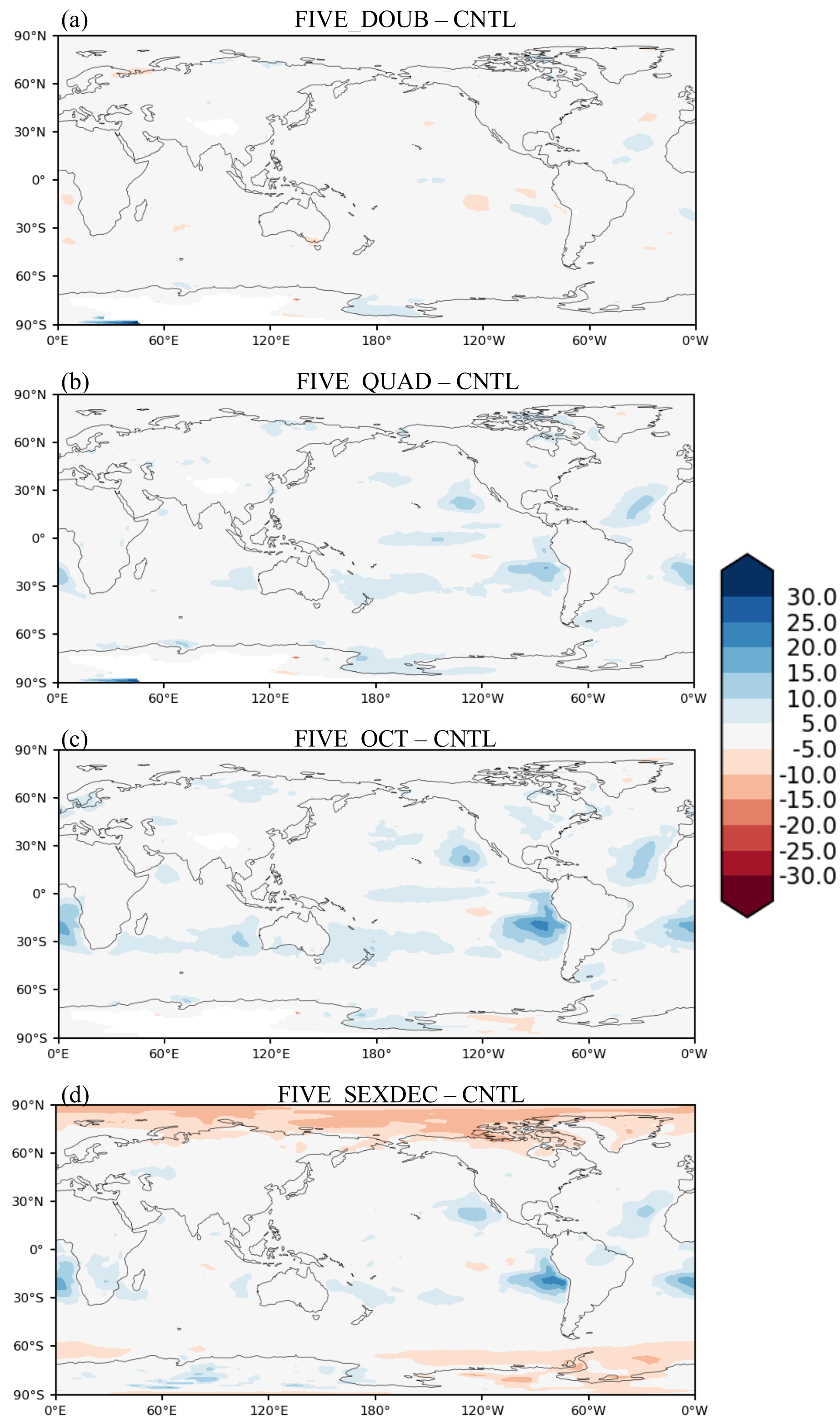

Figure 4. (a) The differences of low-level cloud amount between FIVE_DOUB and CNTL (Figure 2b). (b)-(d) are the same as (a) but for FIVE_QUAD, FIVE_OCT, and FIVE_SEXDEC, respectively.

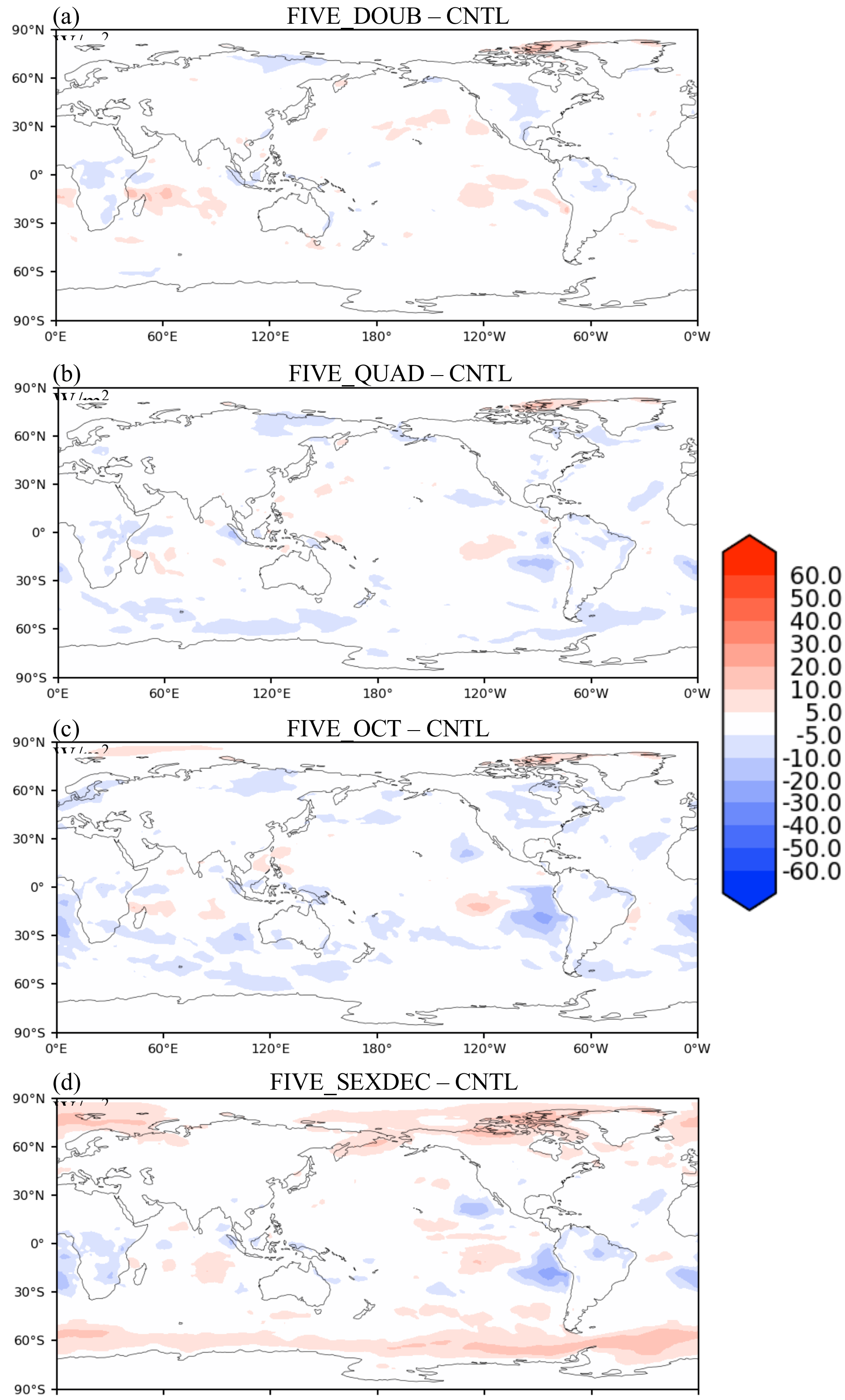

Figure 5. (a) The differences of shortwave cloud radiative effect between FIVE_DOUB and CNTL (Figure 3b). (b)-(d) are the same as (a) but for FIVE_QUAD, FIVE_OCT, and FIVE_SEXDEC, respectively.

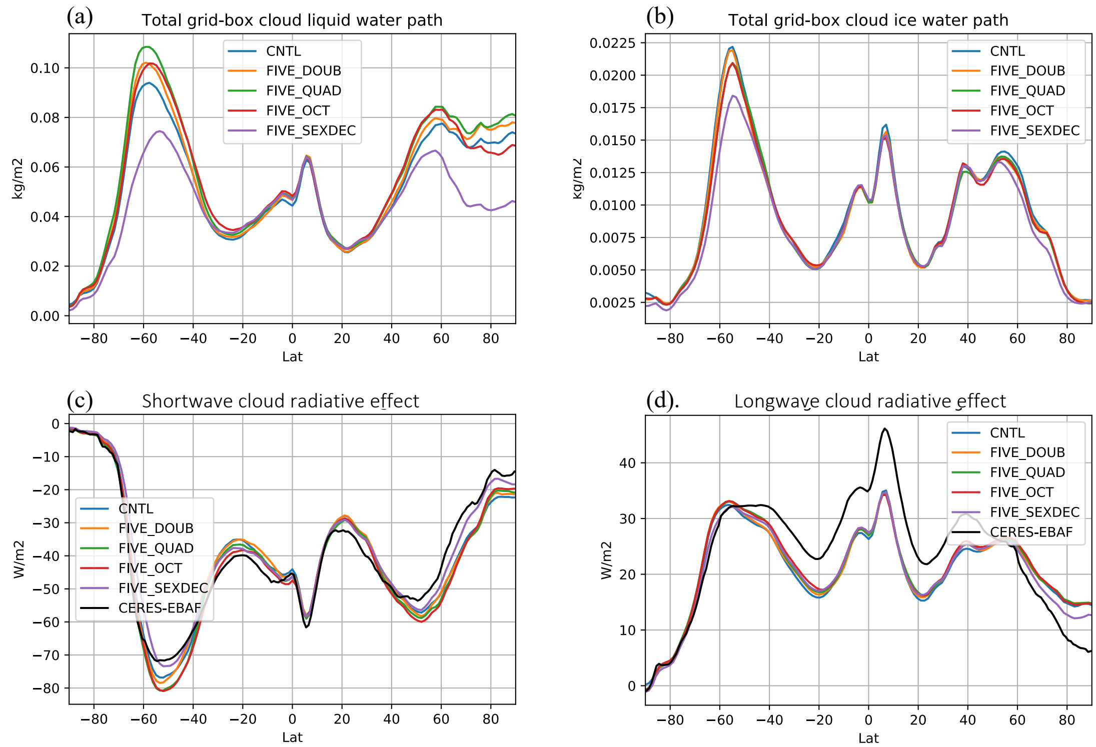

Figure 6. The zonal average of (a) cloud liquid water path (kg/m^2), (b) cloud ice water path (kg/m^2), (c) shortwave cloud radiative effect (W/m^2), and (d) longwave cloud radiative effect (W/m^2) from the simulations of E3SM-FIVE. CERES-EBAF is the Clouds and the Earth's Radiant Energy System (CERES) Energy Balanced and Filled (EBAF) top-of-atmosphere (TOA) data product averaged from 2000 to 2015.

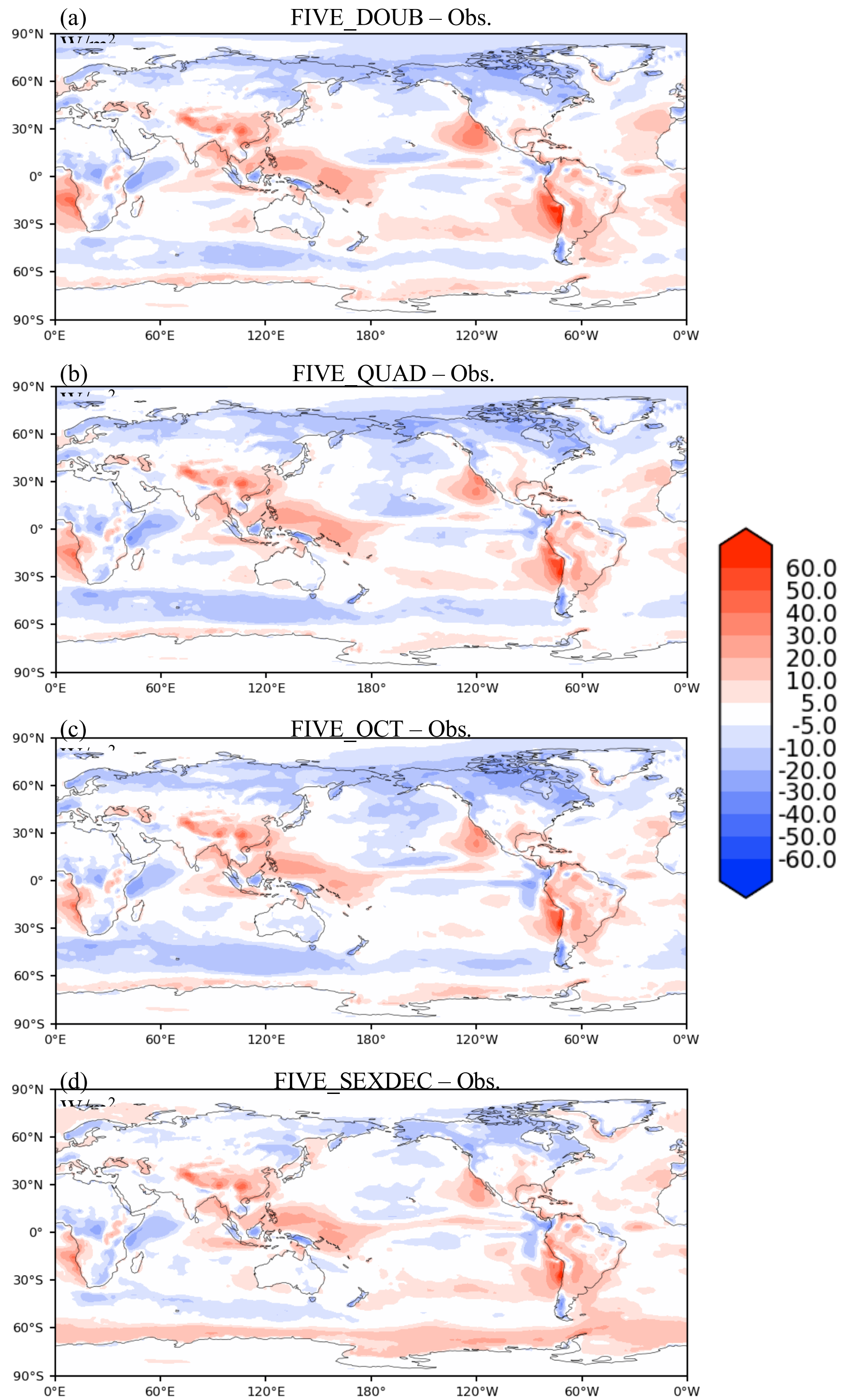

Figure 7. (a) The differences of shortwave cloud radiative effect between FIVE_DOUB and observation (Figure 3a). (b)-(d) are the same as (a) but for FIVE_QUAD, FIVE_OCT, and FIVE_SEXDEC, respectively.

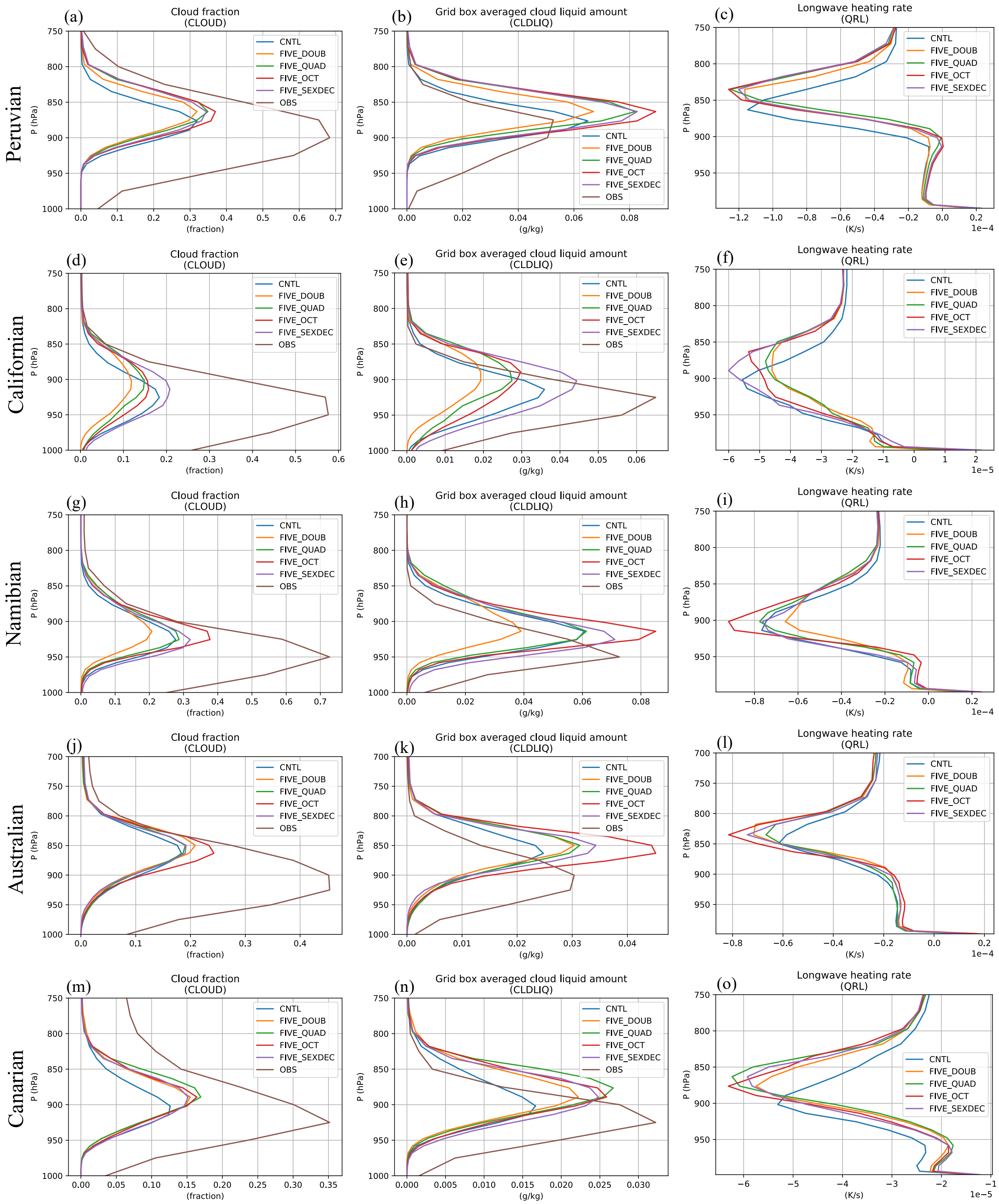

Figure 8. Spatial- and temporal-averaged profiles of (a) cloud fraction, (b) cloud liquid water amount, and (c) longwave heating rate in Peruvian (defined in Table 2) from the simulations of E3SM-FIVE. (d)-(f) are the same as (a)-(c) but in Californian. (g)-(i) are the same as (a)-(c) but in Namibian. (j)-(l) are the same as (a)-(c) but in Australian. (m)-(o) are the same as (a)-(c) but in Canarian.

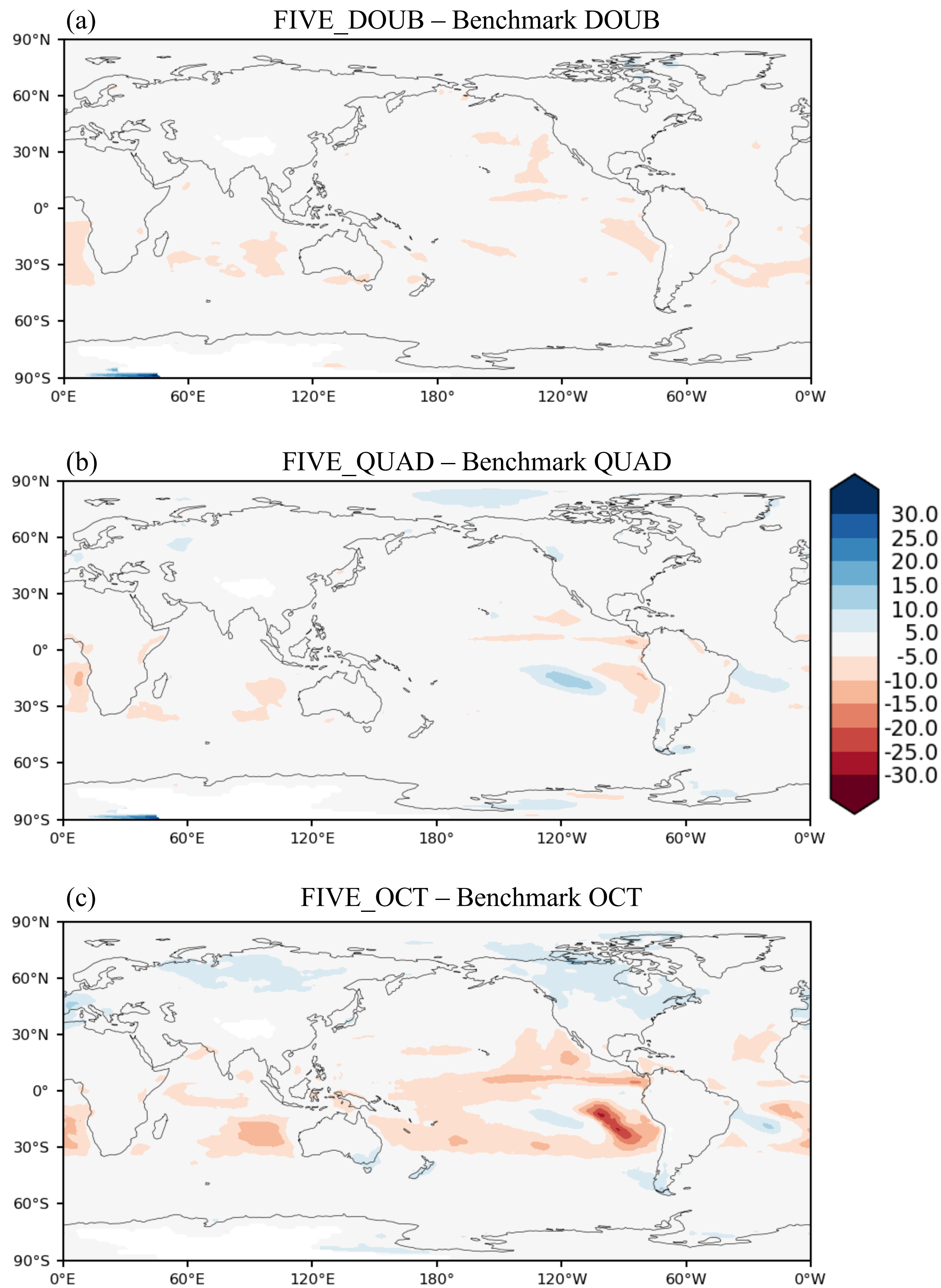

Figure 9. (a) The differences of low-level cloud amount between E3SM benchmark DOUB and FIVE_DOUB (Figure 1b). (b) is the same as (a) but between QUAD and FIVE_QUAD. (c) is the same as (a) but between OCT and FIVE_OCT.

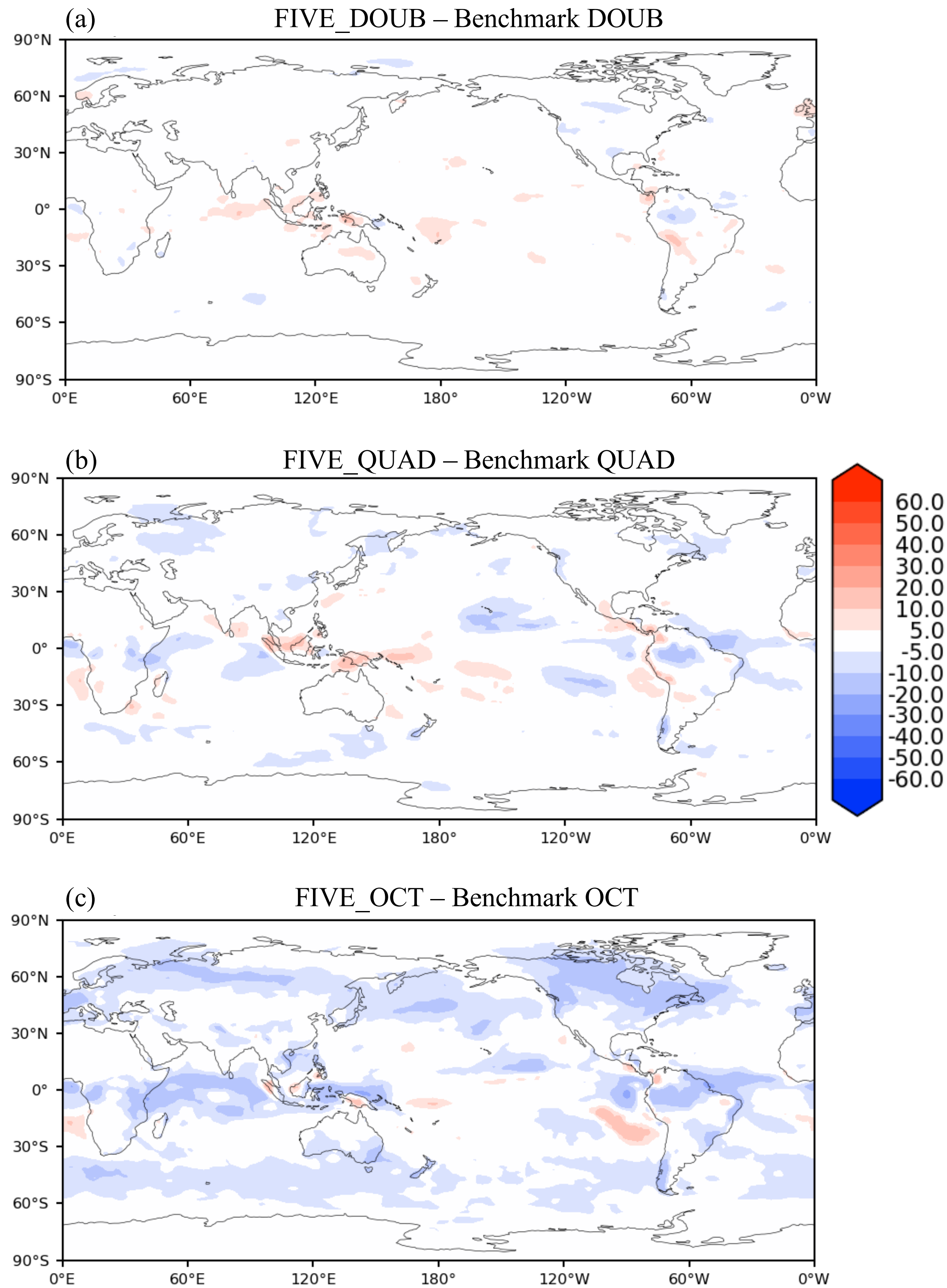

Figure 10. (a) The differences of shortwave cloud radiative effect between E3SM benchmark DOUB and CNTL (Figure 3b). (b) is the same as (a) but between QUAD and FIVE_QUAD. (c) is the same as (a) but between OCT and FIVE_OCT.

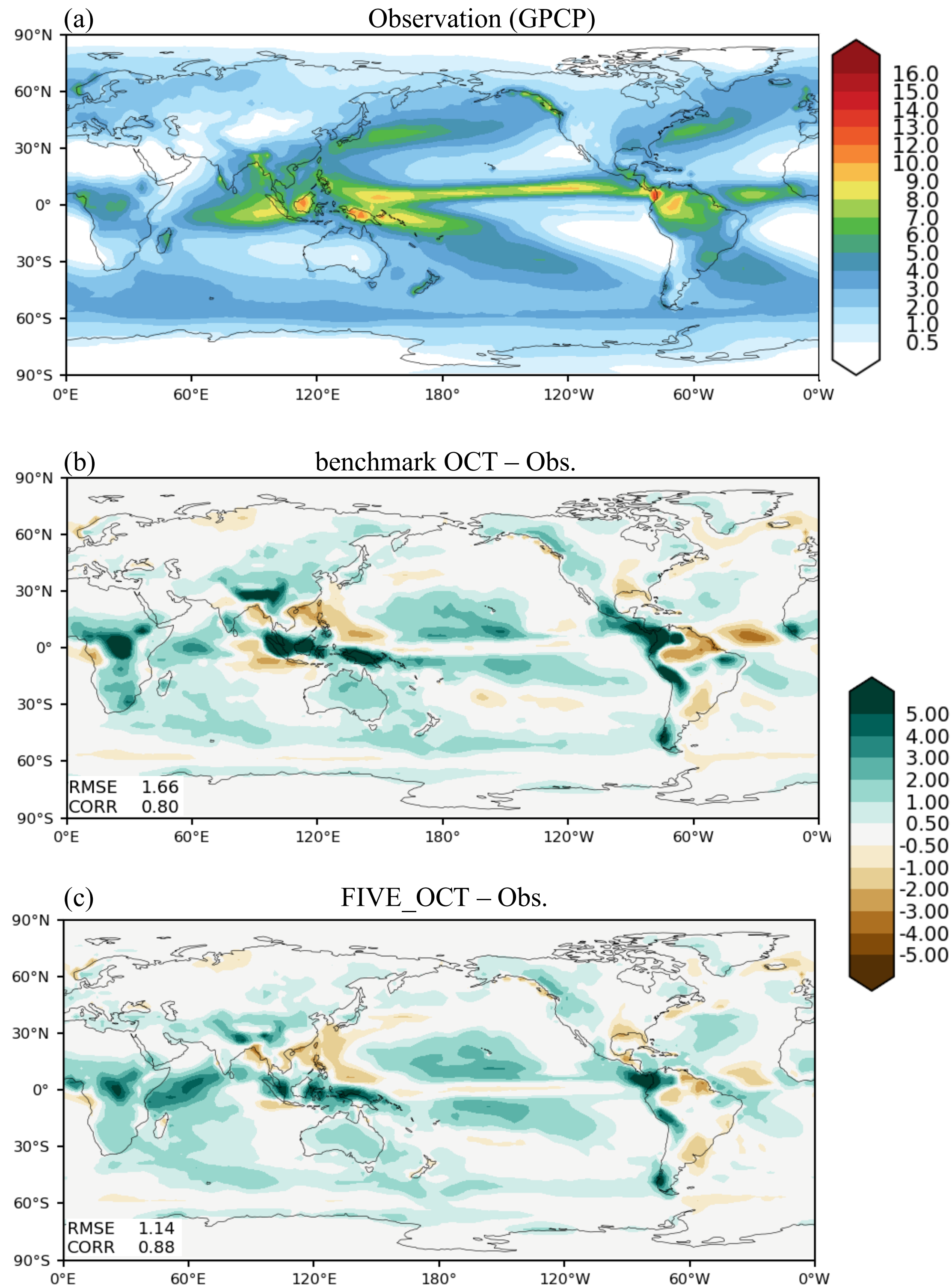

Figure 11. (a) Precipitation from Global Precipitation Climatology Project (GPCP) dataset averaged from 1979 to 2014. (b) The differences of precipitation between E3SM benchmark OCT and observation. (c) The differences of precipitation between FIVE_OCT and observation. The bottom two rows of (b) and (c) display the evolution of the geographical biases, root mean squared errors (RMSE), and correlation coefficients (CORR) of the OCT and FIVE_OCT simulations computed relative to observation.

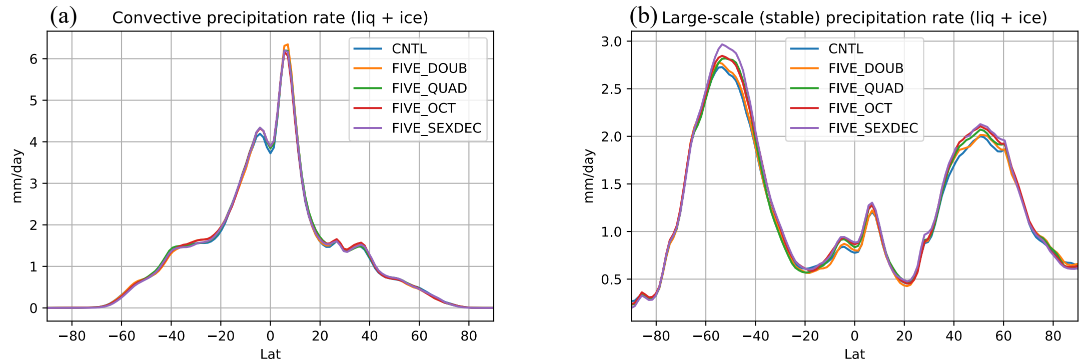

Figure 12. The zonal average of (a) convective precipitation rate (mm/day) and (b) large-scale precipitation rate (mm/day) from the simulations of E3SM-FIVE.

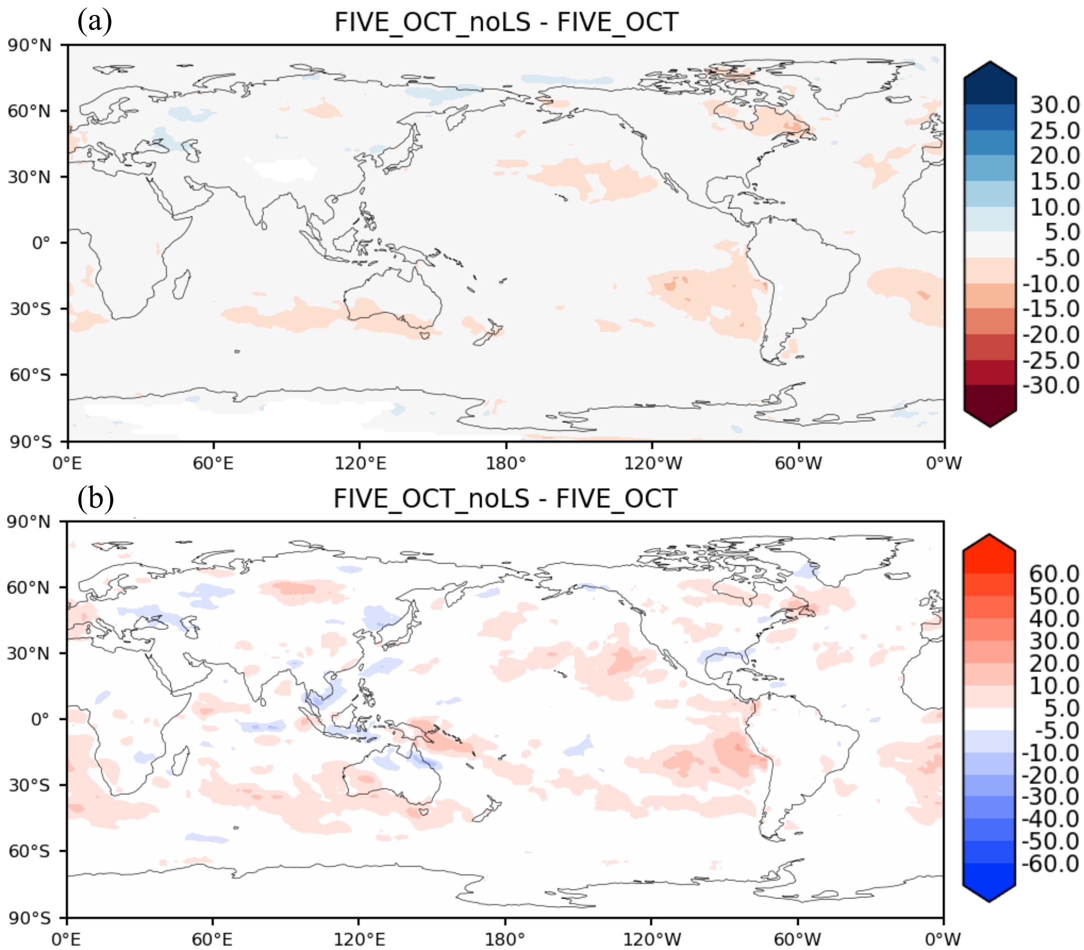

Figure 13. (a) The differences of low-level cloud amount between FIVE_OCT_noLS and FIVE_OCT. (b) The differences of shortwave cloud radiative effect between FIVE_OCT_noLS and FIVE_OCT. The results are two years aveage.

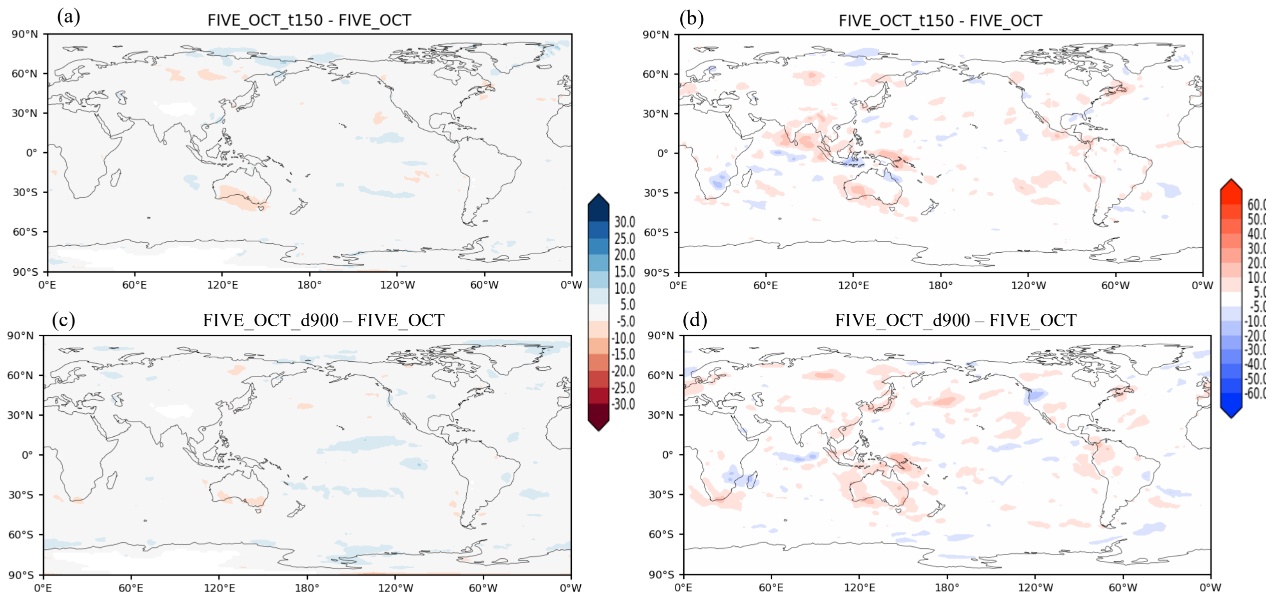

Figure 14. (a) The differences of low-level cloud amount between FIVE_OCT_t150 and FIVE_OCT. (b) The differences of shortwave cloud radiative effect between FIVE_OCT_t150 and FIVE_OCT. (c) and (d) are the same as (a) and (b), respectively, but the differences between FIVE_OCT_d900 and FIVE_OCT. The results are two years aveage.